remote sensing

MDPI

Article

Tracking Moisture Dynamics in a Karst Rock Formation Combining Multi-Frequency 3D GPR Data: A Strategy for Protecting the Polychrome Hall Paintings in Altamira Cave

Vicente Bayarri [1,2], Alfredo Prada [3], Francisco García [4,*], Carmen De Las Heras [3] and Pilar Fatás [3]

[1] GIM Geomatics, S.L. C/Conde Torreanaz 8, 39300 Torrelavega, Spain; vicente.bayarri@gim-geomatics.com
[2] Polytechnic School, Universidad Europea del Atlántico, Parque Científico y Tecnológico de Cantabria, C/Isabel Torres 21, 39011 Santander, Spain
[3] Museo Nacional y Centro de Investigación de Altamira, Marcelino Sanz de Sautuola, S/N, 39330 Santillana del Mar, Spain; alfredo.prada@cultura.gob.es (A.P.); carmen.delasheras@cultura.gob.es (C.D.L.H.); pilar.fatas@cultura.gob.es (P.F.)
[4] Department of Cartographic Engineering, Geodesy and Photogrammetry, Universitat Politècnica de València, Camino de Vera, s/n, 46022 Valencia, Spain
* Correspondence: fgarciag@upv.es

Abstract: This study addresses the features of the internal structure of the geological layers adjacent to the Polychrome Hall ceiling of the Cave of Altamira (Spain) and their link to the distribution of moisture and geological discontinuities mainly as fractures, joints, bedding planes and detachments, using 3D Ground Penetrating Radar (GPR) mapping. In this research, 3D GPR data were collected with 300 MHz, 800 MHz and 1.6 GHz center frequency antennas. The data recorded with these three frequency antennas were combined to further our understanding of the layout of geological discontinuities and how they link to the moisture or water inputs that infiltrate and reach the ceiling surface where the rock art of the Polychrome Hall is located. The same 1×1 m^2 area was adopted for 3D data acquisition with the three antennas, obtaining 3D isosurface (isoattribute-surface) images of internal distribution of moisture and structural features of the Polychrome Hall ceiling. The results derived from this study reveal significant insights into the overlying karst strata of Polychrome Hall, particularly the interface between the Polychrome Layer and the underlying Dolomitic Layer. The results show moisture patterns associated with geological features such as fractures, joints, detachments of strata and microcatchments, elucidating the mechanisms driving capillary rise and water infiltration coming from higher altitudes. The study primarily identifies areas of increased moisture content, correlating with earlier observations and enhancing our understanding of water infiltration patterns. This underscores the utility of 3D GPR as an essential tool for informing and putting conservation measures into practice. By delineating subsurface structures and moisture dynamics, this research contributes to a deeper analysis of the deterioration processes directly associated with the infiltration water both in this ceiling and in the rest of the Cave of Altamira, providing information to determine its future geological and hydrogeological evolution.

Keywords: moisture mapping; Ground Penetrating Radar; 3D modeling; preventive conservation; capillary rise; stratigraphic interpretation; rock art; geomatics

Citation: Bayarri, V.; Prada, A.; García, F.; De Las Heras, C.; Fatás, P. Tracking Moisture Dynamics in a Karst Rock Formation Combining Multi-Frequency 3D GPR Data: A Strategy for Protecting the Polychrome Hall Paintings in Altamira Cave. *Remote Sens.* **2024**, *16*, 3905. https://doi.org/10.3390/rs16203905

Academic Editor: Henrique Lorenzo

Received: 26 August 2024
Revised: 13 October 2024
Accepted: 17 October 2024
Published: 21 October 2024

1. Introduction

The Cave of Altamira, located in Santillana del Mar in the autonomous community of Cantabria in Northern Spain, is a relevant site for human Cultural Heritage, renowned for its prehistoric rock art dating back thousands of years. The cave extends about 290 m and broadens at key locations, most notably the Polychrome Hall, which houses its distinguished paintings and engravings dating from more than 35,000 years ago to 14,000 years ago, including the group of polychrome bison on the Polychrome Hall ceiling (Figure 1).

Altamira holds historical significance as the first cave where Paleolithic rock art was discovered. Its significant archaeological deposits and globally recognized artworks culminated in its designation as a UNESCO World Heritage Site in 1985.

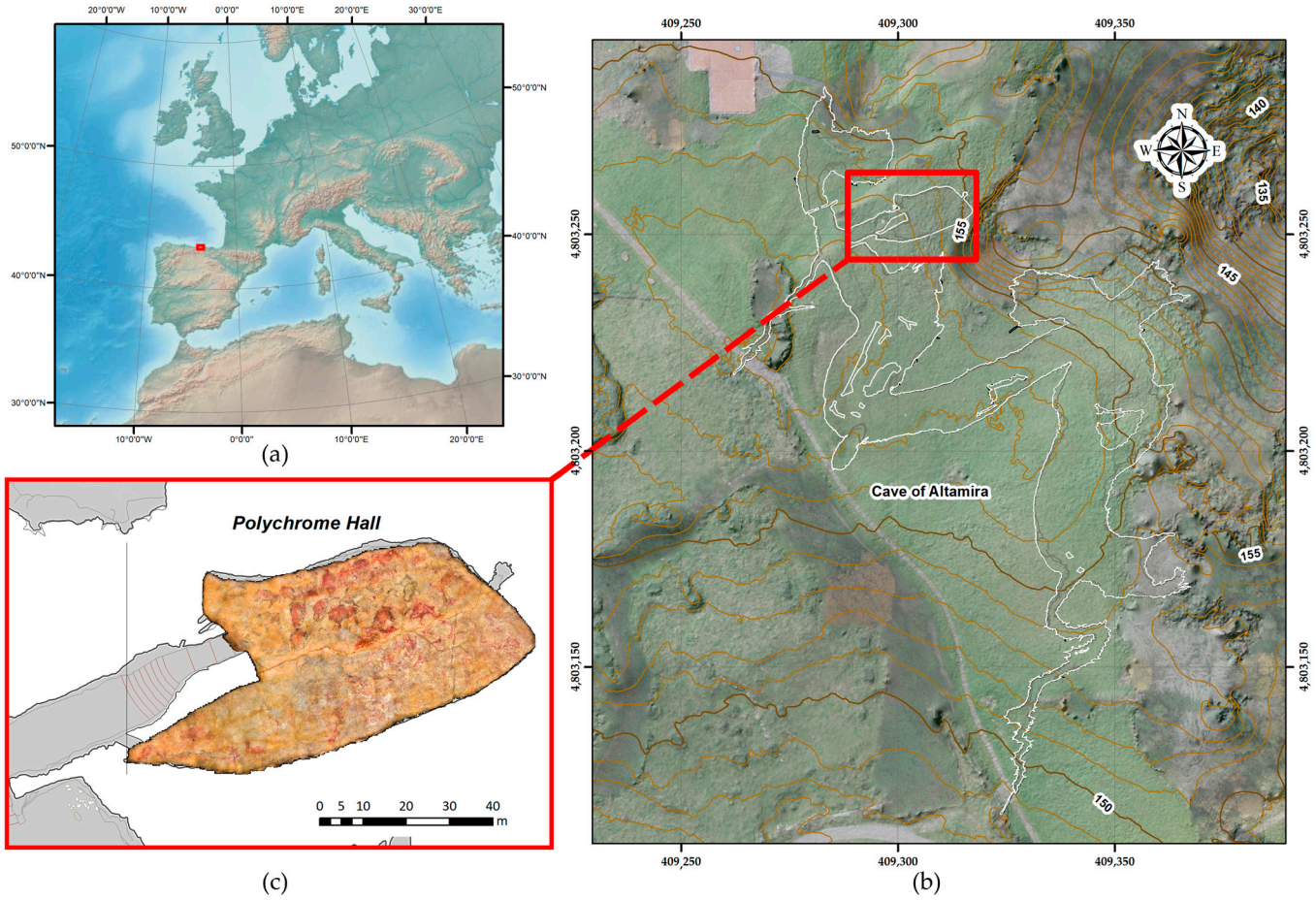

Figure 1. (**a**) Location map of the Cave of Altamira (**b**) Projection of the Cave of Altamira on the orthoimage, indicating in a red frame the position of (**c**) the Polychrome Hall with the rock art orthoimage overlayed.

Over millennia, the cave has served as a recurring site for hunter-gatherer societies, clear in the many representations of animal figures and signs, among other things scattered throughout its halls and galleries a testament to a prolonged artistic creation process. Despite its historical significance, the cave's conservation faces challenges, particularly concerning the conservation of its ancient rock art on the Polychrome Hall ceiling.

The Cave of Altamira is framed within the regional structure of a large syncline called Santillana-San Román, with a NE–SW orientation. The Cave of Altamira began its development in the Pliocene and forms part of the upper zone of a karstic complex. The Altamira Formation is a carbonate series of Cenomanian age (Middle-Upper Cretaceous). The structure and lithology of the Cretaceous calcareous section where the cave is located (Altamira Formation), the reduced strata thickness, with thin marl intercalations, the subhorizontal stratification and its high degree of fracturing mean that gravitational subsidence is one of the most outstanding morphological features. In its present state, the Cave of Altamira can be classified as a senile cave in a phase of dismantling by collapse, with a low development of lithochemical reconstruction processes [1,2]. In particular, the layers that form the overlying strata of the Polychrome Hall, from the ceiling to the ground surface, are as follows [3]:

- Polychrome Layer, consisting of 0.70–0.8 m of whitish-colored limestones. The base of the Polychrome Layer is the ceiling of the Polychrome Hall where the polychrome bison paintings are located.
- Dolomitic Layer, made up of 0.10–0.25 m of highly dolomitized limestone. This Dolomitic Layer is separated from the Polychrome Layer by a loamy-clay intercalation.
- The Fissured Layer, consisting of a 1.3 m package of fissured and karstified limestone.
- Orange Layer, made up of 0.8 m of orange-colored micritic limestones.
- Upper Layer, where 2 m of yellowish limestones and calcarenites with a 0.2 m marly intercalation can be recognized.

The overlying layer, where the bedrock thickness does not exceed nine meters, exhibits signs of brecciation and dissolution, with accumulations of clays and minerals, such as dolomite particles. There is significant decompression both within the Polychrome Layer and in the overlying Dolomitic, Fissured Orange and Upper layers. The structural characteristics of the bedrock have also been altered by the sealing of surface fractures in the Polychrome Layer with Portland cement in the 1920s and 1930s, which likely blocked the direct pathways for rainwater infiltration [4]. In the Polychrome ceiling, water movement is influenced by surface tension, a capillary phenomenon resulting from the physical and chemical properties of water and the inherent porosity of the calcareous rock. This process, characteristic of karstic environments, is crucial in redistributing water through the Polychrome ceiling and contributing to the formation of calcifications and geological structures.

Leading publications in this field [5] underline the importance of collecting key data through remote sensing [6–9] for the safeguarding of Cultural Heritage, with the aim of integrating geospatial analysis with geophysical techniques. The non-invasive feature and high resolutions of geophysical methods allow accurate mapping of discontinuities in geological complexes [10–14]. The use of geophysical methods provides information on the geological environment, helping to improve the results obtained with geological research methods for the study of the internal structure of karst systems [15–20]. Nowadays, Ground Penetrating Radar (GPR) has become the most widely used geophysical tool to pinpoint and locate discontinuities within the rock mass of the karst system, such as fractures, joints, voids, bedding planes and detachments and moisture zones [21–31]. These features make the GPR technique suitable for the study of karst formations with prehistoric art [32–35].

Several GPR campaigns have been conducted with different frequency antennas in 2017, 2018 and 2022, as shown in Figure 2b–e and Table 1, to characterize the real conservation problems affecting the Ceiling, primarily related to the fractures associated with varying depths of water infiltration, which impact the preservation of the rock art [36–39]. These challenges require a deeper understanding of the geological and hydrological processes affecting the cave's stability and rock art preservation. Building on the GPR results of previous campaigns conducted at the Cave of Altamira, a GPR campaign was carried out in April 2023, with the aim of furthering our understanding of the geological and hydrological dynamics within the cave. In this campaign, antennas of different frequencies (Table 1) were used to map the moisture distribution and identify structural features in the rock formations on the ceiling of the Polychrome Hall that support the cave paintings, particularly focusing on the control area designated as ALT1. The aim of this study was to investigate the interaction between moisture infiltration, geological structures, and the preservation of rock art in ALT1. These efforts have yielded significant insights into the spatial distribution of moisture and its correlation with geological features like fissures and microchannels.

In the 2023 campaign, which focused on the multisensory analysis of the moisture course [38], the ALT1 control zone was studied. This ALT1 control zone is located in the center of the ceiling of the Polychrome Hall (Figure 3a). In this control zone there is a prominent Upper Palaeolithic abstract sign: a large red claviform near the hind legs of one of the large polychrome bison.

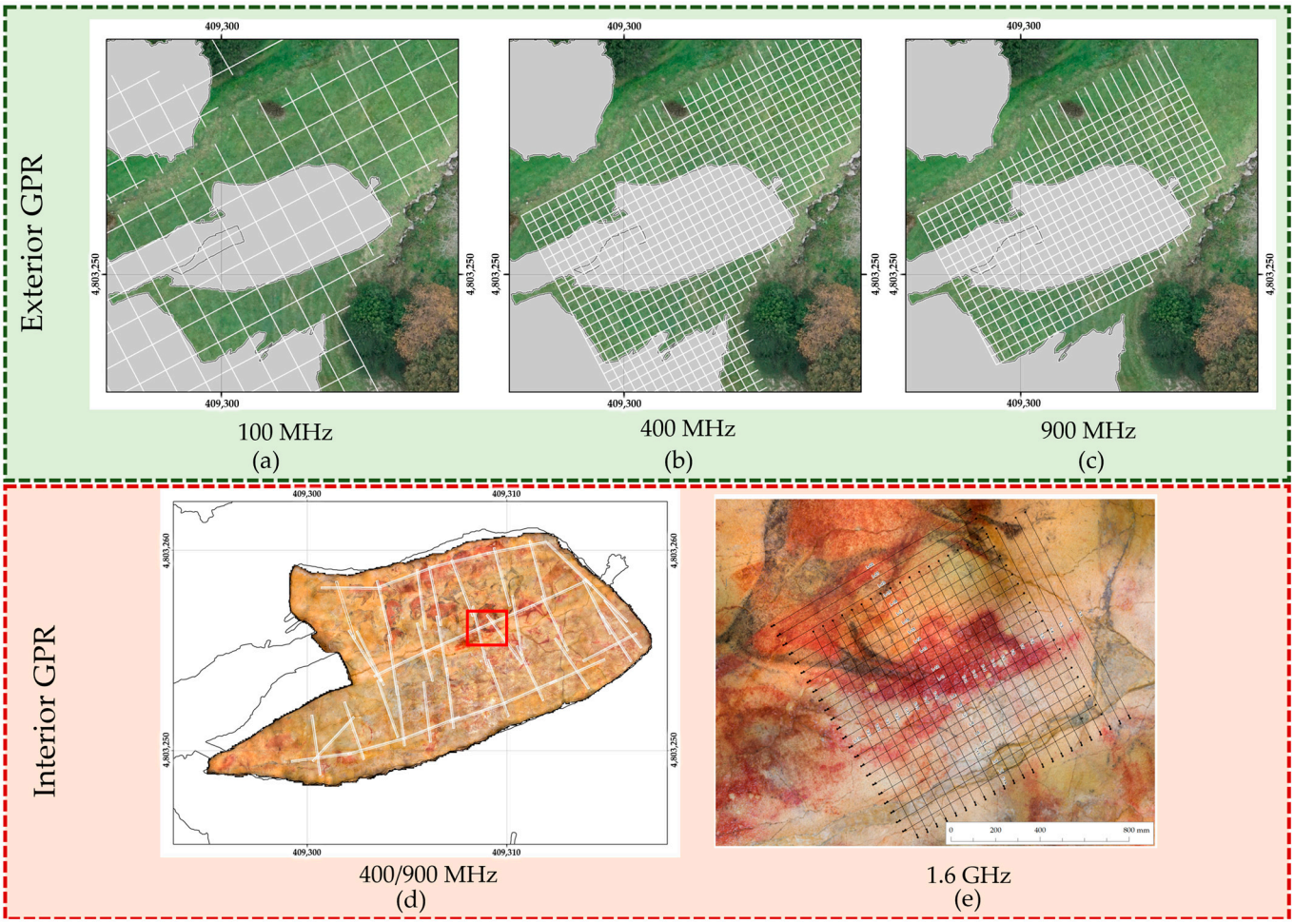

Figure 2. Overview of previous GPR studies conducted in the Altamira Cave and Polychrome Hall ceiling: (**a**) 100 MHz exterior grid 3 × 3 m, (**b**) 400 MHz exterior grid 1 × 1 m, (**c**) 900 MHz exterior grid 1 × 1 m, (**d**) 400 and 900 MHz interior reflection profiles (indicated with white lines), and location of area around ALT1 (indicated with a red square), (**e**) 1.6 GHz interior grid 5 × 5 cm in 2022.

Table 1. Frequency antennas used on the exterior and interior of the Polychrome Hall ceiling of the Cave of Altamira in the different GPR campaigns.

Campaign Year	Cave Exterior Antenna Frequencies	Polychrome Hall Ceiling (Inside the Cave) Antenna Frequencies
2017–2018	900–400–100 MHz	900–400 MHz
2022		1.6 GHz
2023		300–800–1.6 GHz

In the broader scientific landscape, it is well-established that multiple factors drive moisture infiltration into cave environments and impact the preservation of rock art. While some studies emphasize the direct correlation between fissures and moisture ingress, others highlight the role of complex hydrological networks in transporting moisture over vast distances within cave systems, and a third factor considers the impact of condensation water on both water distribution and conservation within these environments.

In the case of Altamira, the three factors are evident: the karst and its dip influence the water supply, the vertical or subvertical fractures provide a direct water supply and condensation water contributes to moisture zones within the cave system.

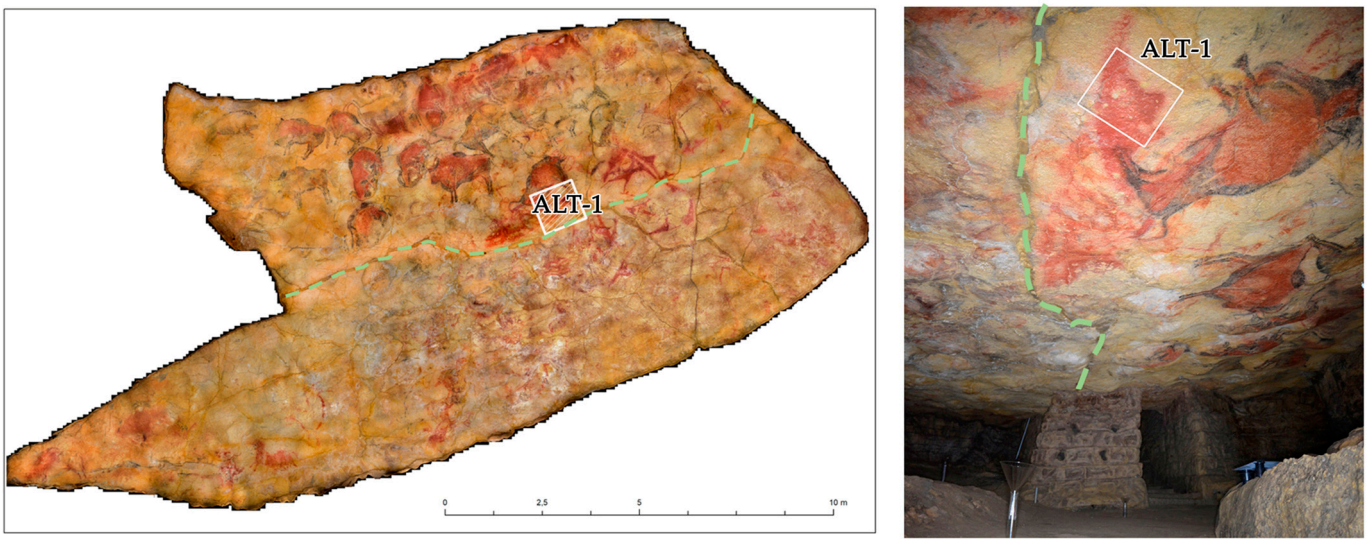

(a) (b)

Figure 3. (**a**) The location of the control area ALT1 on the ceiling of the Polychrome Hall. The dashed light-green line marks the path of the central fracture that runs across the ceiling from west to east. (**b**) A photograph showing a general view of the ALT1 study area, with the same dashed light-green line indicating the central crack, which has been sealed with cement.

This research aims to follow up on previous studies by carrying out a rigorous and detailed analysis of the internal geological structures present in overlaying strata between the outer covering and the cave's ceilings. By using Ground Penetrating Radar (GPR) technique at different frequencies, 300 MHz, 800 MHz and 1.6 GHz as shown in Table 1, we aim to offer the tools to obtain relevant information through non-invasive techniques, highly respectful of the Cave, providing access to internal morphology and detail of relevant areas for conservation concerns. The comparison of antennas used in GPR surveys reveals a balance between resolution and penetration depth (Table 2). The high-frequency 1.6 GHz antenna delivers excellent resolution, able to detect features as small as 2 cm, but it is limited to a penetration depth of approximately 0.4 to 0.5 m [40,41]. On the other hand, the 800 MHz and 300 MHz antennas, while offering lower resolution, can penetrate up to 4 m, making them more suitable for deeper subsurface investigations. This flexibility allows these frequencies to meet conservation objectives by balancing the need for high resolution with the requirement for deeper geological penetration, ensuring effective subsurface imaging and sensing for preservation efforts [42–47].

Table 2. Comparison of the parameters for the 1.6 GHz, 800 MHz and 300 MHz antennas utilized on the ceiling of the Polychrome Hall during the 2023 survey campaign.

Frequency	1.6 GHz	800 MHz	300 MHz
Frequency Range	1.3–1.9 GHz	0.5–1.0 GHz	0.2–0.4 GHz
Wavelength in Air (m)	~0.1875	~0.375	~1.0
Wavelength (m) (ε = 7.5)	~0.0684	~0.136	~0.364
Minimum Resolution (m) (ε = 7.5)	~0.0342	~0.068	~0.182
Estimated Maximum Depth (m) (ε = 7.5) N = 20	~1.1 m	~2.2 m	~6.0 m
Estimated Maximum Depth (m) (ε = 7.5) N = 100	~0.4 m	~0.8 m	~2.0 m
Vertical and Horizontal Resolution	0.0342 m	0.068 m	0.182 m
Image Clarity (Entropy)	0.8–1.0	0.6–0.8	0.4–0.6
Signal Attenuation	High (50–70 dB)	Moderate (30–50 dB)	Low (10–30 dB)
Antenna Gain	High (20–30 dB)	Moderate (15–25 dB)	Low (10–20 dB)
Antenna Beamwidth	15°	30°	45°
Signal-to-Noise Ratio (SNR)	15 dB	10 dB	5 dB

Through analysis and interpretation of GPR data, this study endeavors to provide valuable insights into Altamira geological evolution, structural stability and ongoing conservation challenges. By digging into the processes of deterioration affecting the cave structural stability and indirectly affecting conservation issues related to water infiltration, this research opens the door to implementing preventive measures that guarantee the preservation and sustainability of this Cultural Heritage site, thus, offering a better understanding of some of the most relevant aspects for the conservation of the art of Altamira.

Despite these efforts, there remains a need to further elucidate the geological complexities within the Altamira Cave, particularly focusing on areas like ALT1, which are critical for understanding the interaction between moisture infiltration, geological structures and the preservation of rock art. This study builds on the foundations laid by earlier research campaigns to comprehensively analyze the geological and hydrological dynamics of the Polychrome ceiling in Altamira Cave, offering valuable insights for conservation efforts. This non-invasive geophysical test aims to monitor, by means of 3D mapping, the network of discontinuities (fractures, joints, bedding planes, detachments) and moisture areas present in the overlying layer around the ALT1 control area, from the Upper Layer to the basal surface (Polychrome Layer) of the ceiling of the Polychrome Hall. These factors affect the cave's stability and induce significant changes in the circulation of infiltration water, generating processes of concretion, microcorrosion, dissolution and dragging of paint [48]. This 3D mapping can also provide information on the role played by the water dynamics associated with the monitored section of the central crack (Figure 3), located about 70 cm from our ALT1 control area.

2. Materials and Methods

2.1. Study Area and Design

In the Polychrome Hall, curators have monitored different conservation-sensitive areas. Among these areas is our designated zone, ALT1, in the center of the Polychrome Hall and closely associated with prehistoric paintings, including a prominent sign known as the "claviform" where one of the large polychrome bison is arranged (Figure 4).

The choice of the ALT1 control area within the Polychrome Hall was informed by earlier research indicating microchannels, fractures, and other geological anomalies that could affect the preservation of the paintings. These anomalies facilitated water infiltration, allowing moisture to access the control area through internal fractures.

The study design incorporated campaigns conducted during different seasons or periods of the year to capture temporal variations and assess the long-term dynamics of water infiltration processes associated with the main internal cracks, fractures and fissures within the Polychrome Hall. This seasonal approach helped with the monitoring of changes in moisture distribution, fracture patterns and other geological parameters over time, providing valuable insights into the underlying processes shaping the cave environment and its impact on rock art preservation.

Through the systematic collection of data using Ground Penetrating Radar (GPR) techniques and advanced data processing methods, the study has allowed us to determine the main internal fractures of the ceiling in the ALT1 control area directly involved with the access of seepage water leading to migrations and pigment washing. In addition, this study has helped us to understand in greater detail the internal geological structure directly involved in the stability processes of the rock mass. This interdisciplinary approach aimed to provide a comprehensive understanding of the complex interplay between geological processes, environmental factors and the preservation of this globally significant cave and its rock art.

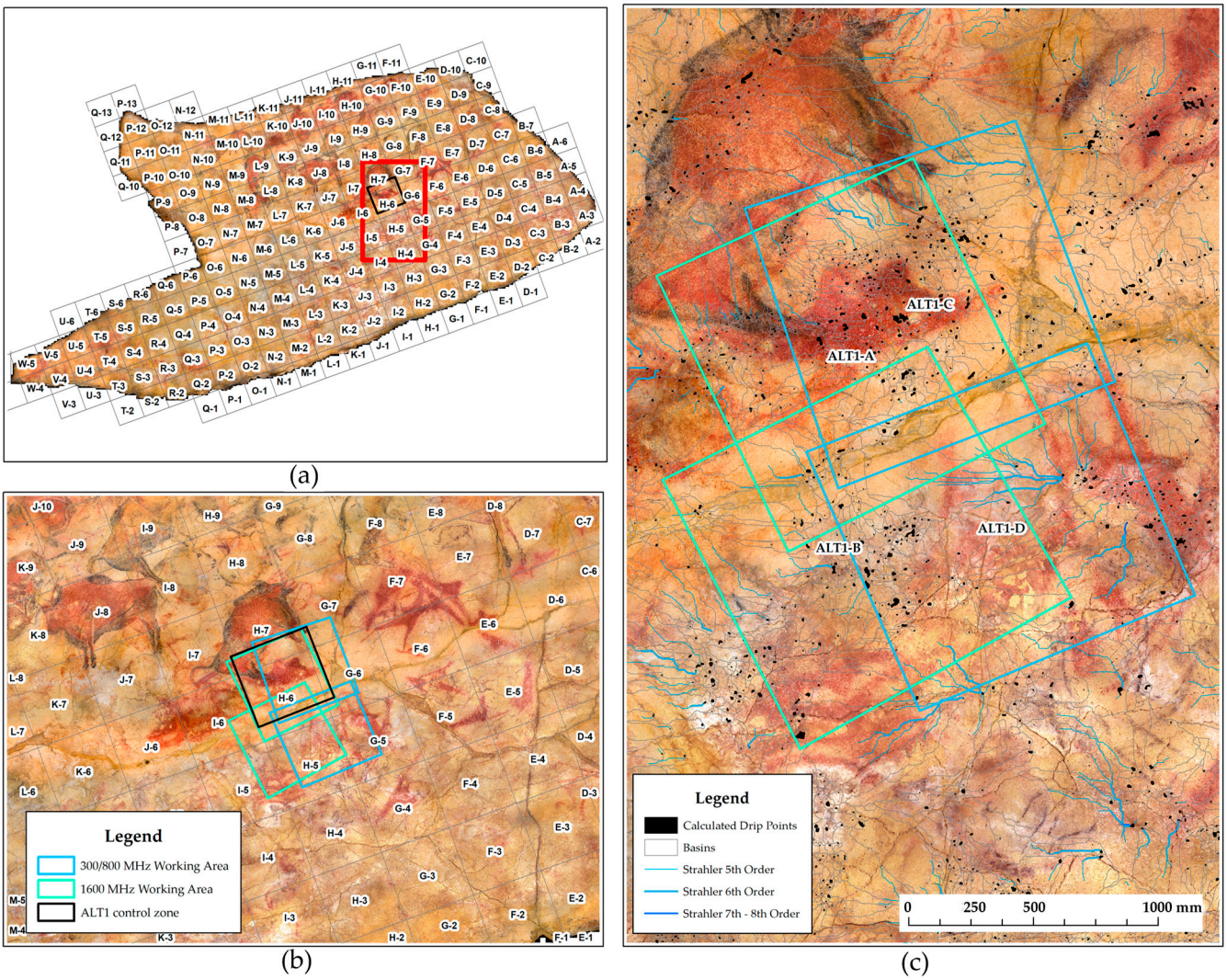

Figure 4. (**a**) Orthoimage of the Polychrome ceiling with the sectorisation grid and the location of the control area ALT1. (**b**) View of the ALT1 control area together with the sectorisation grids and the working areas for the 300/800 MHz and 1.6 GHz antennas and (**c**) overlapping of the working areas for 300/800 MHz and 1.6 GHz antennas with basins, streams and drip points.

2.2. General Workflow Diagram

The data integration process (Figure 5) began with the establishment of a precise reference frame using the Topcon Hyper II [49] (Topcon Corporation, Tokyo, Japan) Global Navigation Satellite System (GNSS) [50,51], which ensured accurate alignment to the European Terrestrial Reference System 1989 (ETRS89). A closed traverse was then carried out using a Topcon GPT-7503 total station (Topcon Corporation, Tokyo, Japan) [52], with 16 stations set out over a distance of 430 m. Checkerboard markers distributed throughout the cave were used for radiation measurements to ensure accurate georeferencing. A 3D model of the cave was then constructed using 3D terrestrial laser scanning (3DTLS) with a Faro Focus X-130 scanner (Faro Technologies Inc., Lake Mary, USA) [53]. This required 300 individual scans and achieved a 95% point adjustment accuracy of 2.7 mm, providing the necessary reference for the photogrammetry process [54,55].

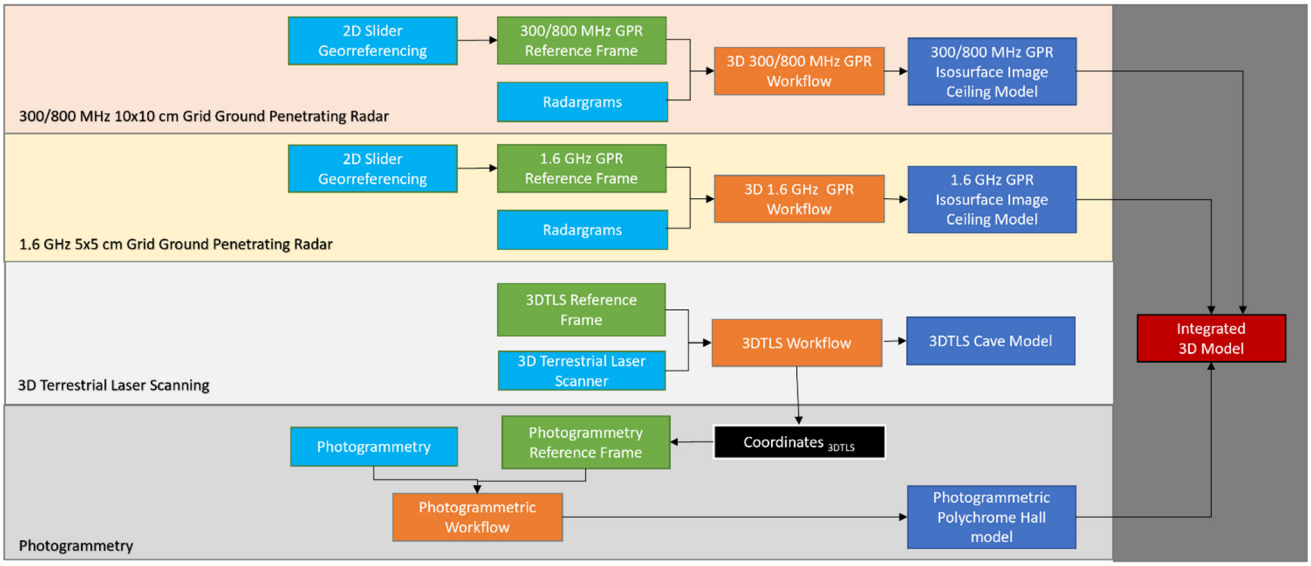

Figure 5. General workflow.

In a previous photogrammetry campaign conducted in 2014 [56], the ceiling of the Polychrome Hall was captured using a Hasselblad H4 D-200 MS camera (Gothenburg, Sweden), achieving a minimum resolution of 16 pixels per mm^2. These images were processed to create a high-density point cloud, which was later refined into a high-resolution 3D digital model of the ceiling. This model enabled the generation of a gigapixel orthoimage and a simplified polygonal model, both of which played an essential role in hydrological calculations to assess water flow patterns and identify possible water infiltration points towards the Polychrome Hall [36–39].

In February 2022, a dual-axis slider system made with three 1.2 m sliders designed to cover a 1 m^2 control area (ALT1) was used in a campaign aimed at estimating the distribution of moisture and discontinuities within the first few centimeters of the support rock where the polychrome paintings are located. A GPR antenna with a central frequency of 1.6 GHz was used to collect 2D radargrams on a 5 × 5 cm orthogonal profile grid, enabling the generation of 3D models, including 3D horizontal slices. The result offered valuable insights into the subsurface conditions that impact the preservation of the paintings.

Building on these findings, a more complete study was conducted in April 2023 using both single and dual-frequency GPR antennas (300/800 MHz and 1.6 GHz). This campaign aimed to further investigate the influence of the central fracture on moisture distribution. The data collection involved adjacent profile grids on either side of the central fracture, with grid dimensions varying according to the frequency used. The slider system ensured precise and consistent data collection during this campaign as well. This study deepened our understanding of the internal structure of the rock mass and its impact on the stability and preservation of the cave's rock art.

2.3. GPR of ALT1 Control Area

2.3.1. GPR Data Acquisition

Ground Penetrating Radar (GPR) was employed as the primary geophysical technique to investigate the subsurface structure and moisture distribution within the Polychrome Hall ALT1 control area. GPR offers a non-invasive and high-resolution method for imaging subsurface features by emitting electromagnetic pulses into the ground and recording the reflections from geological interfaces and moisture content variations.

The GPR surveys were conducted using equipment capable of capturing detailed subsurface images with high spatial resolution, using an SIR 4000 system manufactured by Geophysical Survey Systems, Inc. (GSSI, Nashua, NH, USA). Two GPR antennas (one of them dual) were used to cover a broad range of frequencies and penetration depths,

allowing for comprehensive subsurface characterization with three different resolutions (Table 2):

- 1.6 GHz antenna: This high-frequency antenna was used to capture fine details of the near-surface layers of the ceiling and detect subtle variations in moisture content and geological structures. Its short wavelength provided high-resolution images suitable for mapping fractures, microchannels and other shallow features within the rock formations.
- 300/800 MHz dual-frequency antenna: The dual-frequency antenna provided versatility, enabling deeper penetration into the subsurface while maintaining reasonable resolution. The lower frequency (300 MHz) facilitated imaging of deeper geological interfaces and moisture distributions, documenting moisture zones associated with fractures closer to the surface of the Polychrome ceiling. The higher frequency (800 MHz) offered enhanced resolution for detailed characterization of shallower layer features (discontinuities and moistures) located close to the rock paintings.

Due to the presence of delicate cave paintings on the ceiling of the Polychrome Hall, the GPR data collection was performed using a bow-tie antenna to avoid any physical contact with the artwork, thereby minimizing the risk of damage. The height at which the antenna was positioned had to be carefully managed as it affected the quality of the data. To mitigate this effect and maintain the required minimum ceiling clearance, the data acquisition heights were adjusted according to the antenna frequency. For the dual frequency 300/800 MHz antenna, the height was set to 20 cm (Figure 6a), and for the 1.6 GHz antenna, it was lowered to 10 cm (Figure 6b). However, the irregularities of the ceiling, characterized by pronounced protrusions, caused the distances to fluctuate. In some areas, the antenna was positioned as close as 10 cm, while in other areas the distance was greater, requiring continuous verification to ensure safe clearance. These antenna heights optimized energy transfer into the rock mass and reduced air coupling effects, which was critical to obtaining high quality GPR data [57,58]. The setup allowed penetration depths of up to 50 cm with the 1.6 GHz antenna, 2.8 m with the 800 MHz antenna and 4.3 m with the 300 MHz antenna, while maintaining high-resolution imaging capabilities [40,44,59]. The GPR surveys were conducted using a dual-axis slider system equipped with three 1.2 m sliders, designed to cover a 1 m^2 control area (Figure 6). This system ensured controlled movement and consistent data collection along predefined trajectories. During data acquisition, consistent survey parameters such as antenna orientation and odometry were maintained. The slider position was 3D scanned to accurate georeferencing and spatial registration of the data.

During data collection, the GPR system operated in continuous-wave mode, emitting electromagnetic pulses into the subsurface at regular intervals along the survey lines. Simultaneously, the system recorded the amplitude and travel time of reflected signals, capturing detailed information about subsurface features, interfaces and moisture content variations.

To ensure comprehensive coverage and reduce data gaps, the GPR profiles were spaced closely, with overlapping regions between adjacent lines. A 300/800 MHz antenna was used on the slider with a 10 × 10 cm equidistance grid (Figure 7a), while a 1.6 GHz antenna was employed with a 5 × 5 cm equidistance grid (Figure 7b). This setup facilitated precise mapping of internal fractures and potential water infiltration points, crucial for understanding rock mass stability and preserving the cave's rock art.

To enhance data quality and reduce noise interference, consistent antenna positioning, orientation and scan speed were maintained throughout data acquisition. These measures were crucial in achieving high-resolution subsurface profiles and 3D models.

(**a**) (**b**)

Figure 6. Photographs showing the GPR data collection set-ups in control area ALT1. (**a**) with the 300–800 MHz dual-frequency antenna and (**b**) with the 1.6 GHz antenna.

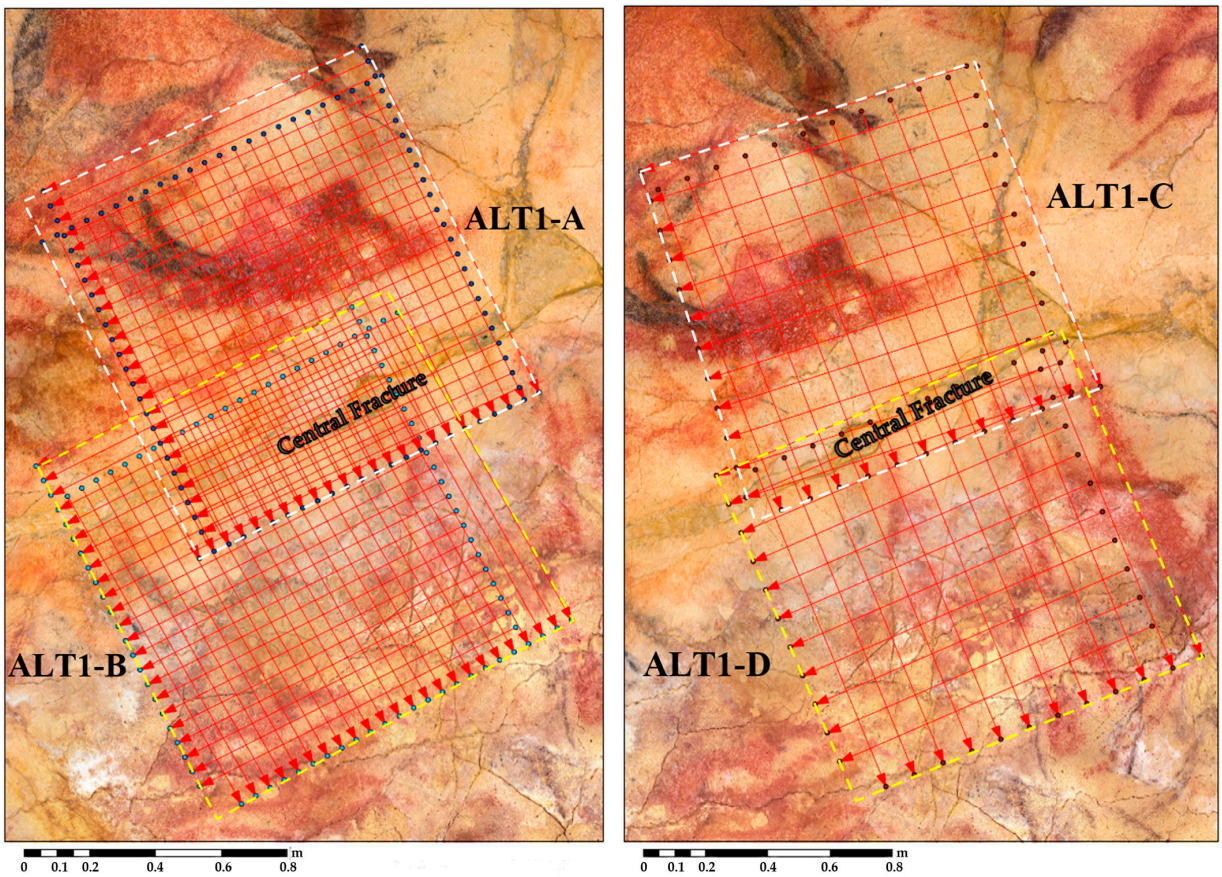

Figure 7. (**a**) Location of the two grids with an equidistance of 5 cm of the profiles using the 1.6 GHz antenna in the study areas ALT1-A (in white dashed square) and ALT1-B (in yellow dashed square). (**b**) Location of the two 10 cm × 10 cm grids using the 300/800 MHz dual frequency antenna in the study areas ALT1-C (in white dashed square) and ALT1-D (in yellow dashed square).

2.3.2. Data Processing

The processing of the GPR field data has followed the processing steps for A-scan, B-scan and C-scan of the GPR signal that were performed in the previous campaigns [37,38]. The use of the Hilbert transform (instantaneous amplitude) attribute in the interpretation of GPR data allows for increased understanding of the internal structure of the Polychrome Layer by characterizing the electromagnetic response to moisture zones within the layer over time. In addition, articles [37,38] describe the various factors, including discontinuities, that influence the amplitude of the electromagnetic wave. Furthermore, these considerations of how the instantaneous amplitude can be equivalent to the moisture content distribution and what other factors can also cause changes in amplitude have been based on contributions from several authors [12,31,46,47,60–71].

The average GPR wave velocity was determined using the hyperbolic fitting method on a series of hyperbolas recorded across different reflection profiles for the three-frequency antennas. This resulted in a mean velocity of 0.111 m/ns. The dielectric permittivity (ε) was calculated to be 7.2, following the low-loss media equation described in [60,62,72]. This velocity was then used for time-to-depth conversion and Kirchhoff migration during the 2D processing of the GPR data.

The raw GPR data obtained from the three different antennas underwent post-acquisition processing before amplitude maps were created and 3D images were generated from the reflection profiles. Basic processing steps were applied to the raw data, followed by a Hilbert transform attribute (instantaneous magnitude) using RADAN 7.6 software (Geophysical Survey Systems, Inc., GSSI, Nashua, NH, USA) [73]. Initially, 1D processing was performed, starting with zero-time correction. Then, 2D processing was applied to the reflection profiles, which included the following: (i) background removal; (ii) bandpass filtering; (iii) application of linear amplitude gains; (iv) Kirchhoff migration with the calculated mean velocity (0.111 m/ns); (v) time-to-depth conversion using the same mean velocity and (vi) Hilbert transform attribute for instantaneous magnitude. Once processed, each reflector profile was aligned within the grid to generate horizontal 3D amplitude maps and isosurface images that helped to identify significant moisture/water zones. Amplitude slice maps were created at different depths, revealing subsurface moisture/water features to depths of 50 cm with the 1.6 GHz antenna, 2.8 m with the 800 MHz antenna and 4.3 m with the 300 MHz antenna. These depth-slice maps allowed for the identification of moisture-rich areas at fixed depths. After generating the depth maps, the highest amplitude values from all profiles were plotted on an isosurface image. This image was color-coded to emphasize the highest amplitudes, while lower values were rendered transparent, simplifying the visualization and interpretation of the main moisture/water zones in the surveyed ceiling strata.

Data quality assessment procedures, such as visual inspection of refraction profiles, signal-to-noise ratio analysis and comparisons with ancillary data (e.g., surface topography and geological surveys) were used to identify and correlate contact layers in the GPR data according to geological stratigraphy [60,62,74].

3. Results

The interpretation of GPR data has revealed significant findings that contribute to our understanding of the Polychrome Hall ceiling geological structure and hydrological processes involved in the conservation of painting. In addition, complimentary datasets, such as basins, streams, drip points, cracks and fractures (Figure 8), were integrated with the results of the GPR data to help with a comprehensive interpretation and analysis. This interdisciplinary approach enabled the identification of subsurface structures, moisture dynamics and geological features relevant to the study objectives. Thus, the interpretation of the GPR results involved the qualitative and quantitative analysis of subsurface images, identification of geological interfaces and characterization of moisture content variations.

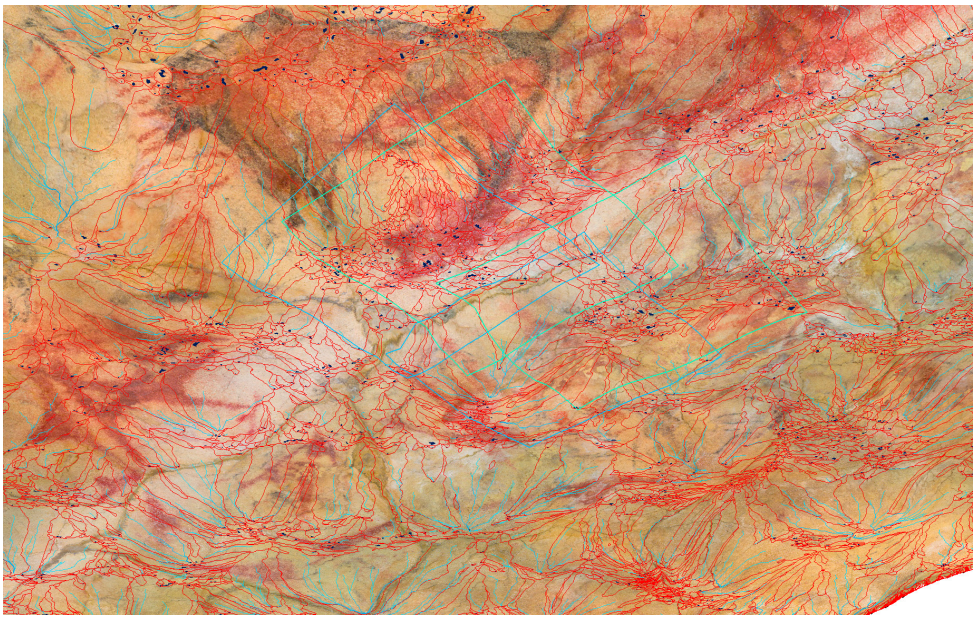

Figure 8. 3D model including basins (in red), streams (in light blue), drip points (in black) and the working areas (green boxes) for 1.6 GHz and 300/800 MHz antennas.

3.1. Detection of Subsurface Features

The GPR survey conducted in the Polychrome Hall enabled the detection and characterization of various subsurface features crucial for understanding the ceiling geological and hydrological dynamics (Figure 9). The interpretation of GPR data revealed diverse features, including fractures, geological interfaces, sedimentary layers and moisture related to discontinuities directly related to the supply of moisture or infiltration water to the uppermost layers of the Polychrome ceiling.

Fractures and fissures were prominently identified throughout the surveyed, taking into account their orientations, lengths and degrees of connectivity area at different depth penetration ranges according to the frequency antennas used (Figure 9b–e). These features reflect the complex tectonic history and structural framework of the cave system. The distribution and density of fractures not only provide insights into the mechanical properties of the rock mass but also indicate potential pathways for fluid migration and small dragged deposits of the type of clay particles, quartz, limestone, etc. within the subsurface environment, considering their dip and involvement in moisture-related discontinuities in the study area.

Moreover, the GPR data facilitated the mapping of geological interfaces, such as bedding planes, joints and contacts between different lithological units (Figure 9b–d). These interfaces play a significant role in delineating the geological stratigraphic architecture of the cave and can influence overlying layer flow patterns and the distribution of moisture within the subsurface layers.

Sedimentary layers, including limestone deposits, were discerned from the GPR data, allowing for the characterization of the depositional history and lithological heterogeneity within the cave. The identification of sedimentary sequences provides valuable information for reconstructing past environmental conditions and interpreting the geological evolution of the cave system.

Furthermore, the GPR survey facilitated the detection of moisture-related zones, such as areas of high moisture content, water infiltration zones and points of active dripping. These zones are indicative of localized hydrological processes, including percolation, condensation and capillary rise, which influence the distribution of moisture on the surface of the Polychrome ceiling. Understanding the spatial variability of moisture dynamics is crucial for assessing the preservation of rock art and geological formations.

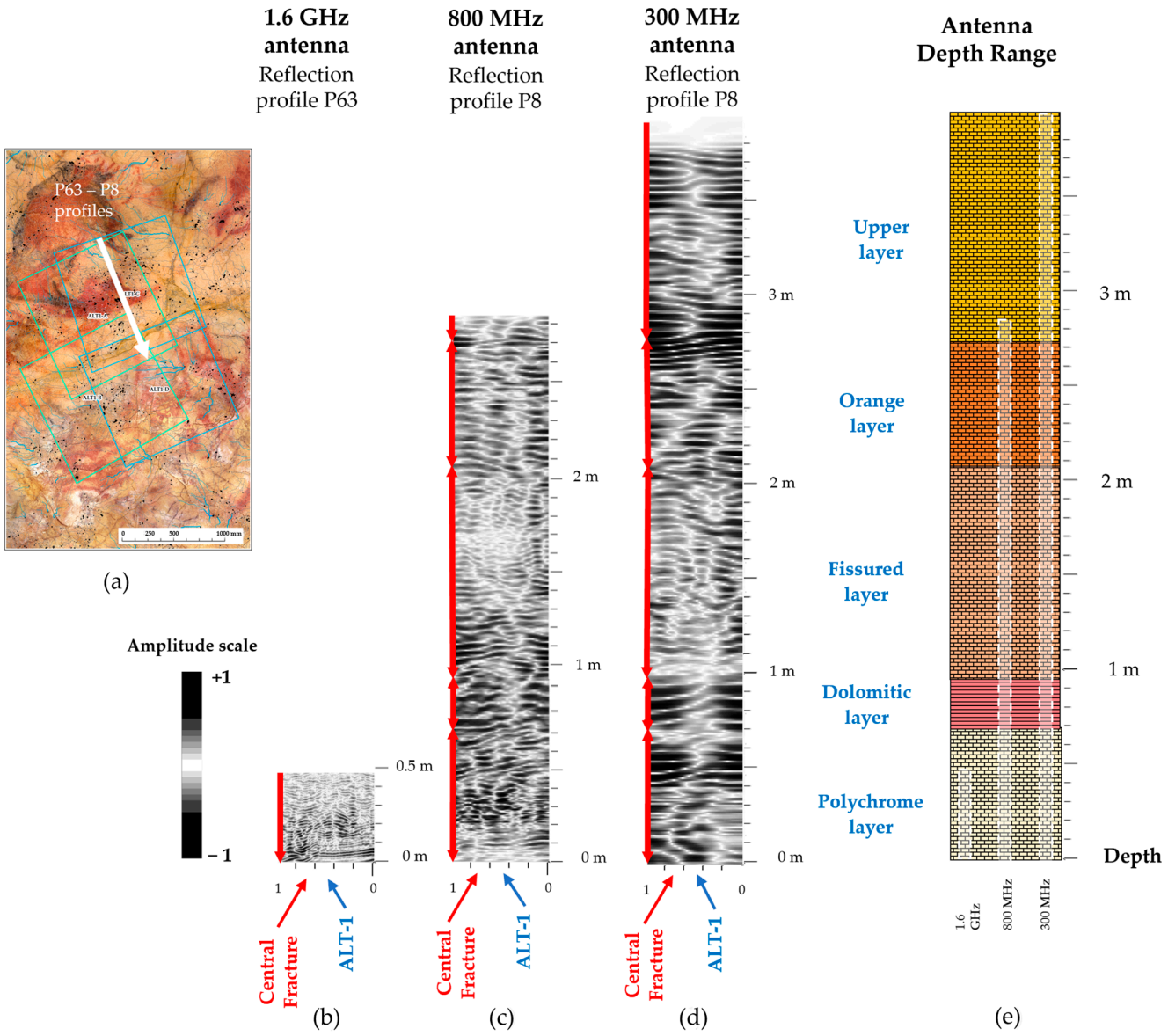

Figure 9. GPR reflection profiles processed in the ALT1 control area showing the main subsurface features (discontinuities), in particular the central fracture, with their stratigraphic correlations of the overlying layers of the ceiling for each frequency antenna used: (**a**) Location of P63 and P8 profiles which spatially coincide, (**b**) reflection profile P63 antenna 1.6 GHz; (**c**) reflection profile P8 antenna 800 MHz; (**d**) reflection profile P8 antenna 300 MHz; (**e**) schematic stratigraphy of the Polychrome Hall ceiling according to [2,3], showing the depth range reached with the 1.6 GHz, 800 MHz and 300 MHz frequency antennas.

3.2. Characterization of Moisture Dynamics

The GPR data analysis enabled a comprehensive characterization of moisture dynamics within the studied area of the Polychrome Hall ceiling, shedding light on the spatial distribution, temporal variability and hydrological processes governing moisture movement within this specific part of the cave environment.

The area of moisture directly implicated with the pigment drip points at ALT1 and recorded by the 1.6 GHz antenna in February 2022 was at a depth of 3 cm from the Ceiling surface. The survey carried out on 26 April 2023, with the same antenna, and for the same control area, relates a series of moisture zones at a depth of 9 cm from the Ceiling surface, with the one described above from the February 2022 campaign (Figure 10). This being a first approximation, and considering the need to obtain new data for different

periods, we propose that there is a dynamic in terms of water infiltration that, through the fractures, fissures and internal stratification planes, percolates to the surface of the Ceiling. We consider that the internal moisture zones mapped in our ALT1 control area on 17 February 2022 has had an impact, from April of the same year, on the washing of pigment in the drip points within the ALT1 control area, as well as causing the migration of paint in other associated drip points. In addition, the moisture zone recorded in April 2023 at a depth of 9 cm and above was directly involved in the paint washing processes at the same drip points and possibly others in April 2024.

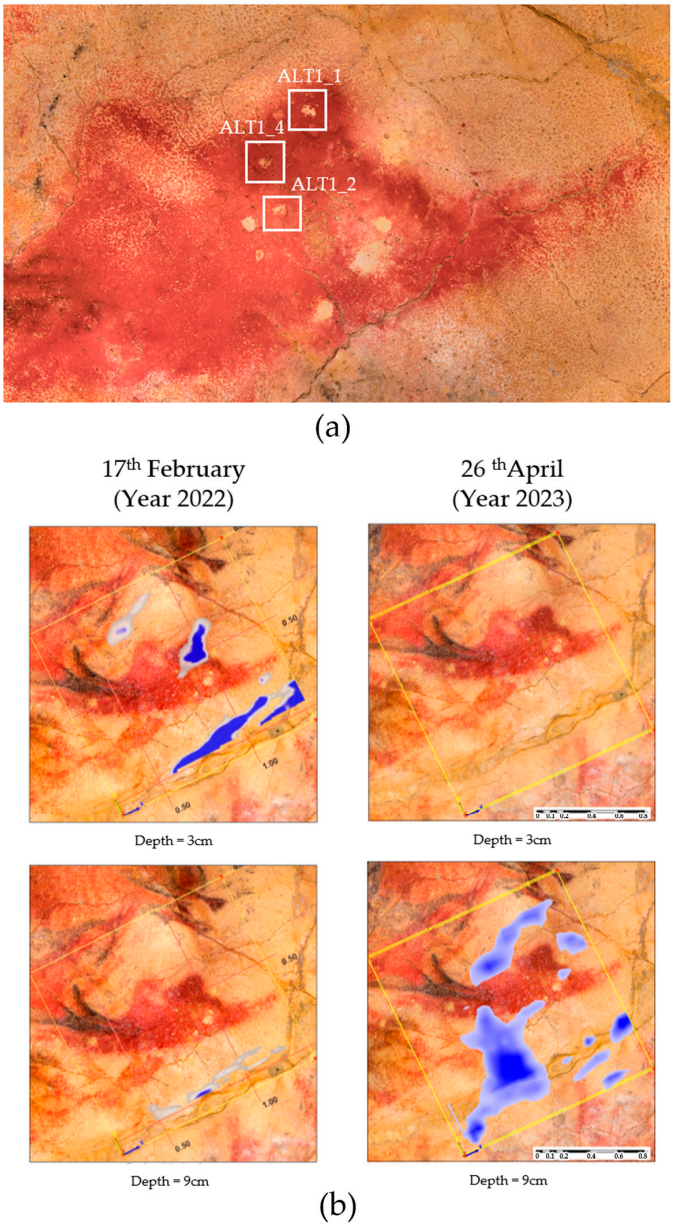

Figure 10. (**a**) location of the drip points ALT1_1, ALT1_2 and ALT1_4 involved in migration and pigment loss within the control area ALT1. (**b**) Evolution of the internal moisture zones detected by the 1.6 GHz antenna directly involved in the above mentioned dropping points.

In addition, it is likely that the moisture zone recorded in April 2023 at a depth of 9 cm and above is responsible for some of the pigment loss associated with the drip points located in ALT 1 that were recorded in April 2024. Further data collection over different time periods is needed to refine these observations and better understand the dynamics of moisture affecting the cave rock art.

Furthermore, the GPR analysis provided insights into the temporal variability of moisture content within ALT1 control area, including how this influences the degradation processes of the paint. By conducting repeated surveys at different time intervals, changes in moisture depths over time can be monitored. This approach allows for the identification of seasonal fluctuations, short-term hydrological events and long-term trends in moisture infiltration and redistribution. Understanding the temporal dynamics of moisture infiltration is important for assessing the vulnerability on the preservation of the paintings and its relation to the degradation processes that lead to microcorrosion of the supporting rock and, consequently, to the loss of adhesion of the pigment that generates the migration and washing away of the pigment. It also reveals internal changes, such as the reservoir effect of moisture, where saturation in one area can lead to water access in other internal areas, akin to a communicating vessels effect.

Additionally, the GPR survey facilitated the characterization of moisture retention zones and storage reservoirs within the subsurface environment. By identifying areas with high moisture content and delineating their spatial extent, the survey highlighted regions where water accumulates and persists over time. These moisture retention zones play a critical role in sustaining cave ecosystems, supporting microbial communities and influencing the growth of speleothems and other calcite deposits, while also inducing microcorrosion processes in combination with the accumulation or concentrations of CO_2, largely originating from the outside vegetation near the cave [75].

The GPR data offered valuable insights into how moisture dynamics interact with the cave's rock art features. By correlating moisture anomalies with the distribution of paintings, the survey highlighted potential impacts of moisture infiltration on the conservation of the existing art in this control area. Understanding these interactions is crucial for developing conservation strategies aimed at preserving the cave art, particularly on the ceiling of the Polychrome Hall, where moisture infiltration poses a significant risk to its preservation (Figure 11).

Figure 11. South area of the ceiling of the Polychrome Hall affected by carbonate concretions produced by the access of seepage water through the fracture zones.

3.3. Mapping of Geological Interfaces

The GPR survey provided detailed mapping of geological interfaces within the Polychrome Hall, offering insights into the subsurface structure and stratigraphy of the cave system.

One of the primary outcomes of the GPR analysis was the delineation of stratigraphic boundaries present in this area of interest and their correlation with the geological layers of the cave. By analyzing the reflections from subsurface interfaces, the survey identified distinct layers corresponding to different lithological units, such as limestone and dolomite. These stratigraphic boundaries are crucial for understanding the geological history of the cave, including depositional processes, sedimentary sequences and tectonic events that have shaped the landscape over time.

Furthermore, the GPR data revealed the presence of structural features such as fractures, faults and joints that intersect the geological layers within the cave. These structural discontinuities play a significant role in controlling the flow of water, gases and nutrients through the subsurface environment.

Moreover, the mapping of geological interfaces enabled the identification of karst features such as dissolution cavities, conduits and void spaces within the limestone bedrock. These karst features are critical components of the cave hydrological system, serving as conduits for groundwater flow and reservoirs for water storage. By delineating the spatial extent of karst features, the GPR survey contributed to the understanding of overlying layer flow patterns, recharge mechanisms and hydrological connectivity within the cave network.

Additionally, the GPR data facilitated the characterization of sedimentary deposits and alluvial fill within the overlying layer. By mapping the distribution and geometry of sedimentary layers, the survey enhanced our understanding of overlying layer sedimentology, including sediment transport mechanisms, depositional environments and paleoenvironmental reconstructions.

3.4. Correlation with Previous Studies

Comparing the findings of the current GPR survey with earlier studies conducted in the Polychrome Hall ceiling provided valuable insights into the temporal and spatial variability of subsurface features and moisture dynamics within the overlying layer system. The GPR survey results were compared with data obtained from earlier studies, revealing both consistencies and discrepancies between the findings. This comparative analysis shed light on the dynamic nature of the cave environment and the limitations of individual survey techniques.

One notable part of the correlation analysis was the confirmation of previously identified geological interfaces and structural features within the cave. The GPR data corroborated the existence of stratigraphic boundaries, fractures and karst features reported in earlier studies, showing the reliability and reproducibility of the survey methodology. This consistency in the identification of subsurface features across different studies enhances confidence in the interpretation of cave hydrogeology and geological processes.

However, discrepancies between the current GPR results and earlier findings were also seen, particularly regarding the spatial distribution and intensity of moisture dynamics within the cave. While earlier studies may have provided qualitative descriptions or localized measurements of moisture content, the GPR survey offered a more comprehensive and quantitative assessment of subsurface moisture patterns. Discrepancies in moisture dynamics between the current study and earlier investigations may arise from differences in survey resolution, data interpretation techniques or temporal variations in environmental conditions, water distribution and internal moisture.

The correlation analysis highlighted the importance of temporal monitoring and multi-methodological approaches in overlying layer research. By integrating data from multiple surveys conducted over different time periods and using diverse techniques, researchers can gain a more holistic understanding of the dynamics of the moisture bathing the ceilings of the Cave, especially the Polychrome Ceiling, and improve the accuracy of

environmental assessments. To further corroborate the data, future studies could enhance the analysis by correlating external precipitation processes with the time factor and their internal accumulation through fracture lines.

As for the specific moisture dynamics seen within the ALT1 area, direct correlation was made with the points of pigment dripping (Figure 10a) recorded by the 1.6 GHz antenna in February 2022. This moisture, previously at a depth of between 3 and 5 cm, is documented months later at a greater depth some 9 cm above its previous position. This observation indicates a significant shift in moisture distribution over time, with implications to preserve cave art. The analysis suggests that moisture present in February 2022 contributed to the washing of pigment dripping points in April, May and June 2022, and the current moisture depths, documented in April 2023, are slightly higher and have affected the pigment close to the drip points associated with our control area ALT1, as well as other control areas separated by a few centimeters from it (ALT12) in April 2024. This reflection underscores the dynamic nature of moisture infiltration and its potential effects on the conservation of cave art over successive years (Figure 12).

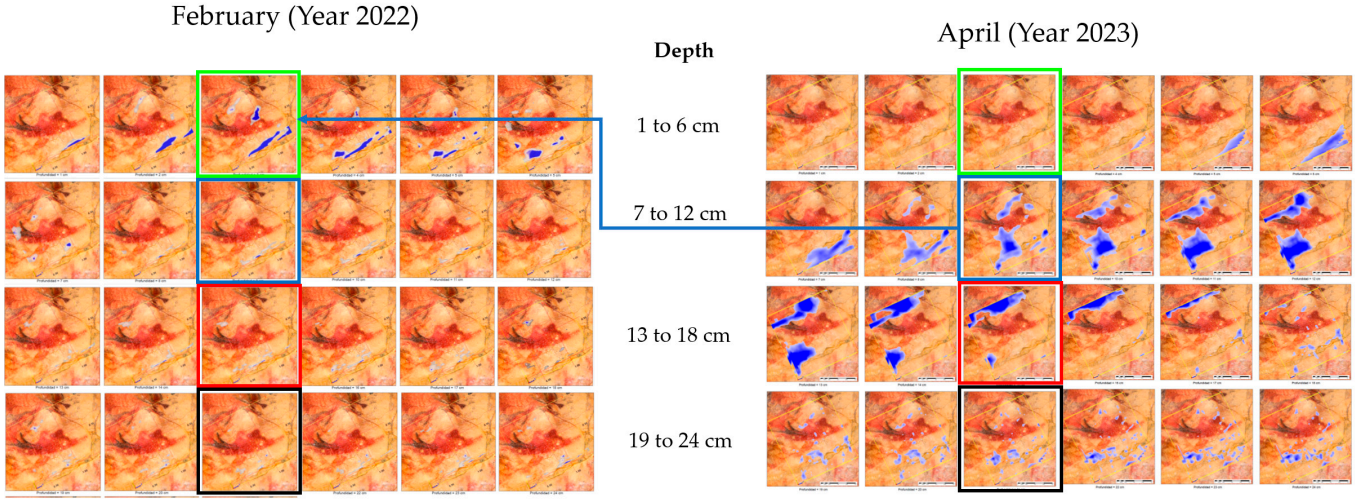

Figure 12. Evolution of moisture in the ALT1 control area. The highlighted boxes indicate significant changes in moisture depths relative to depth. In February 2022, higher moisture zones were observed at lower depths, while in April 2023, lower moisture zones were recorded at lower depths. The moisture recorded between April and June, which was involved in paint drips, has already reached the surface of the Ceiling; therefore, it was not detected by the 1.6 GHz antenna on 26 April 2023. The blue arrow connects the moisture moisture zones that, year after year, are associated with pigment dragging drips in ALT1.

3.5. Antennas Comparison

The comparison between different antennas operating at frequencies of 1.6 GHz, 800 MHz and 300 MHz provided valuable insights into the subsurface features of the Polychrome Hall within the Cave of Altamira. Each antenna frequency offered unique advantages and limitations, contributing to a comprehensive understanding of the geological and hydrological dynamics within the cave environment.

1.6 GHz Antenna: This antenna showed superior resolution, allowing for detailed imaging of shallow subsurface features with high precision. This antenna frequency proved effective in delineating fine-scale geological structures and moisture anomalies within the ALT 1 control area of Polychrome ceiling. By capturing subtle variations in moisture content and stratigraphic boundaries, the 1.6 GHz antenna helped with the identification of preferential flow pathways and moisture retention zones critical for understanding hydrological processes affecting the conservation of the art on the ceiling of the Polychrome Hall.

800 MHz Antenna: The 800 MHz antenna offered a balance between resolution and depth penetration, providing intermediate-level imaging of subsurface features within

the Polychrome Hall. This antenna frequency captured broader geological features and moisture patterns compared to the 1.6 GHz antenna, enabling the visualization of both shallow and moderately deep subsurface layers. While lacking the resolution of the higher-frequency antenna, the 800 MHz antenna provided valuable information on the spatial distribution of moisture and geological structures at a more extensive scale.

300 MHz Antenna: The 300 MHz antenna excelled in depth penetration, allowing for imaging of deeper subsurface layers and geological structures within the cave. While sacrificing resolution compared to the higher-frequency antennas, the 300 MHz antenna provided valuable insights into the stratigraphy and hydrogeological dynamics of the cave environment at greater depths. This antenna frequency was effective in mapping large-scale geological features and identifying potential subsurface water reservoirs or flow channels critical for understanding long-term moisture dynamics within the cave.

Integrating data from all three antennas provided a comprehensive view of the subsurface environment within the Polychrome Hall, complementing each other's strengths and compensating for individual limitations. The 1.6 GHz antenna was critical for understanding the dynamics of water flow and its direct impact on paint in the ALT1 control area, revealing the relationship between moisture and surface fissures and fractures. Meanwhile, the 800 MHz and 300 MHz antennas provided valuable insights into deeper subsurface structures. Specifically, the 800 MHz antenna helped correlate the detailed information from the 1.6 GHz antenna with larger fractures and structural features, while the 300 MHz antenna elucidated how these deeper fractures relate to external water entrance. By combining data across these frequencies, we developed a nuanced understanding of the geological and hydrological processes affecting the cave environment, which informs more effective conservation strategies and management decisions.

3.6. Integration with Other Data Sources

Integrating GPR data with other data sources is critical for a comprehensive understanding of the processes affecting the conservation of the art in the cave, especially the one on the ceiling of the Polychrome Hall. Ground truth measurements and field observations, collected during geological surveys and hydrological monitoring campaigns, serve as essential reference points.

In this sense, the observations made by [48] conclude that the ceiling surface of the Polychrome Hall is characterized by a discontinuous and irregular clay film, occasionally carbonated, situated between the limestone substrate and the paint layer. Internal stresses within these clays, induced by moisture variations (wetting/drying cycles), lead to the loss of adhesion of the pigment to the clay layer, and consequently, to the substrate. Concurrently, environmental humidity contributes to carbonate dissolution, as the accumulation of water films on the limestone surface promotes mineral decomposition reactions [76].

The adhesion loss of the pigment to the substrate is further linked to the physicochemical properties of the infiltrating water, which, through the soil cover, incorporates CO_2 and other nutrients from the soil [3]. This process partially dissolves the limestone, resulting in the formation of small, interconnected depressions on the ceiling, resembling a hydrographic network. These depressions act as conduits for transporting not only the paint but also carbonates, salts, clays, quartz fragments, dolomite and other materials, dragging them towards various drip points [77].

The interpretations derived on the one hand from the GPR data which inform us of the important relationship in the inner part of the Ceiling of the fracture lines with the accumulations of moisture (Figure 13). The samples of sediments and pigment dragged from the drip points (Figure 14), corroborate the hypotheses outlined in the previous paragraph.

Visual inspection with a binocular magnifier, along with Scanning Electron Microscope (SEM) and X-ray diffraction analysis of pigment samples and other water-transported deposits at the drip points in ALT1, reveals millimeter-scale particle detachment indicative of flaking, disintegration or loss of cohesion. Additionally, SEM analysis has identified particles with low iron content and high concentrations of magnesium, calcium and oxygen,

likely corresponding to dolomite-type minerals associated with the Dolomitic Layer above the Polychrome Layer. The Dolomitic Layer is affected by a network of discontinuities extending from its roof to its walls, compromising the waterproofing of the thin loamy-clay intercalation separating it from the Polychrome Layer. These discontinuities help with the movement of water and moisture from the upper layers to the Polychrome Layer, aggravating the pigment detachment and rock degradation observed in the Hall.

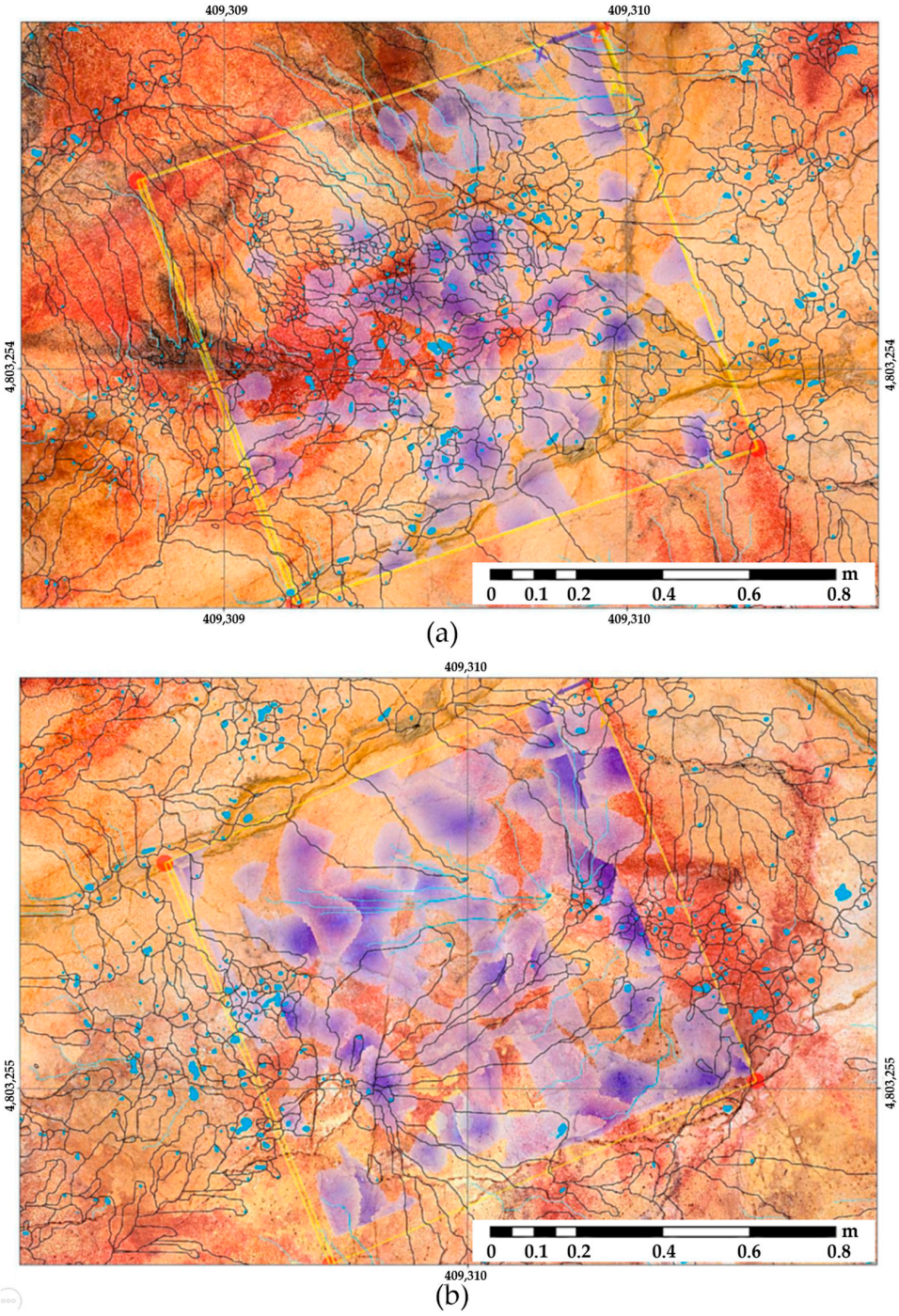

Figure 13. Overlying of the 3D horizontal sections framing the Dolomitic Layer in the 70 cm to 100 cm depth interval in the ALT1-C zone, captured using a 1.6 GHz GPR antenna. The figure shows multiple zones of irregularly distributed moisture, projected on the ceiling surface of the Polychrome Hall with the micro-basins and with the active drip points (water/moisture zones in shades of purple; active drip points in blue) for zones (**a**) ALT1-C and (**b**) ALT1-D.

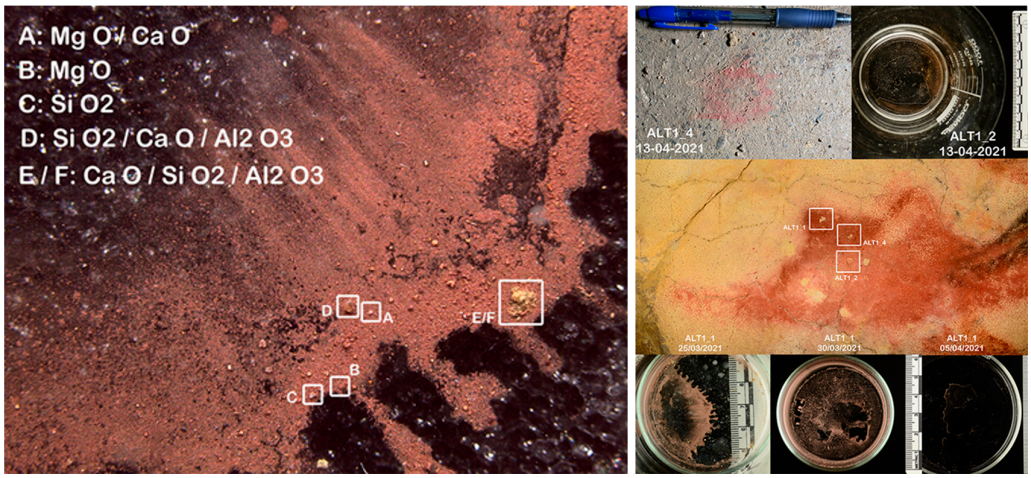

Figure 14. Pigment particles and other mineral deposits carried away by the drip water and collected in the containers located on the ground perpendicular to the drip points. SEM analysis of the detached particles indicates the existence of microcorrosion processes of the supporting rock associated with the presence of infiltration water, condensation and CO_2 concentration.

Moreover, the integration of GPR data with high-resolution surface models, basin, streams, drop points and orthoimagery enables the spatial context of subsurface features to be visualized and analyzed within the broader landscape context. Georeferenced GPR profiles overlaid on topographic maps or DEMs provide valuable insights into the relationships between surface morphology, hydrological pathways and subsurface structures, facilitating the identification of geological controls on ceiling evolution.

Furthermore, the integration of GPR data with hydrological models enables the assessment of long-term trends and predictive modeling of groundwater flow dynamics. This complex system of discontinuities represents the main pathways of fluid exchange with the interior of the Polychrome Hall (Figure 15), as well as with the seepage from the active drip points on the basal surface of the Polychrome Layer in the ALT1 control area (Figure 10a).

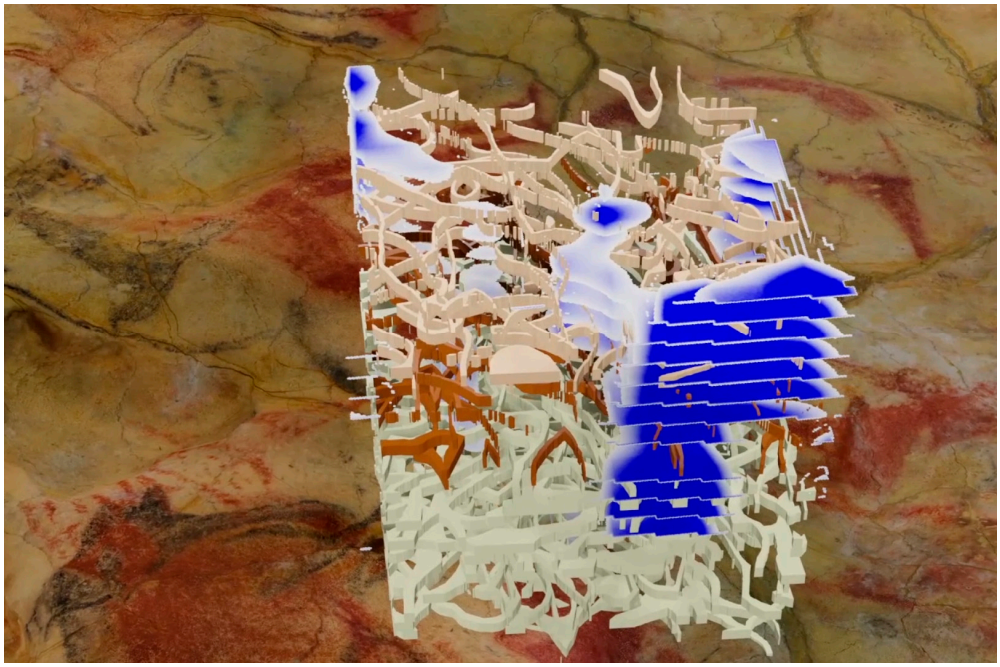

Figure 15. Perspective view of the discontinuities revealing zones of higher moisture, represented by a blue to white gradient, across the different strata of the Polychrome ceiling. Data were collected

using three GPR antennas: a 1.6 GHz antenna for the upper 50 cm, an 800 MHz antenna for depths up to 1.2 m, and a 300 MHz antenna for depths up to 4.9 m. This complex network of discontinuities highlights the primary pathways for fluid exchange within the interior of the Polychrome Hall, as well as seepage from the active drip points located on the basal surface of the Polychrome Layer in the ALT1 control area.

4. Discussion

The findings in this study provide valuable insights into the subsurface features of the Polychrome Hall within the Altamira Cave, as revealed by GPR surveys.

The different geophysical prospecting campaigns (February 2022 and April 2023) on the surface of the ceiling in the ALT1 control area indicate that the presence of moisture of infiltration water is mainly related to two lateral contributions, one on the south side, clearly associated with the large central fracture, and the other on the north side from a fracture similar in development to the central one, which even begins at a higher level (barely one meter above the surface) and which, in a discontinuous manner, practically reaches the surface of the Polychrome Hall. Another fracture on the north side has a similar development to the central one, beginning at a higher level (barely one meter from the surface) and discontinuously reaching the ceiling surface, vertically aligned with the belly and hind legs of the bison located near the claviform sign in our control area ALT1 (Figure 16).

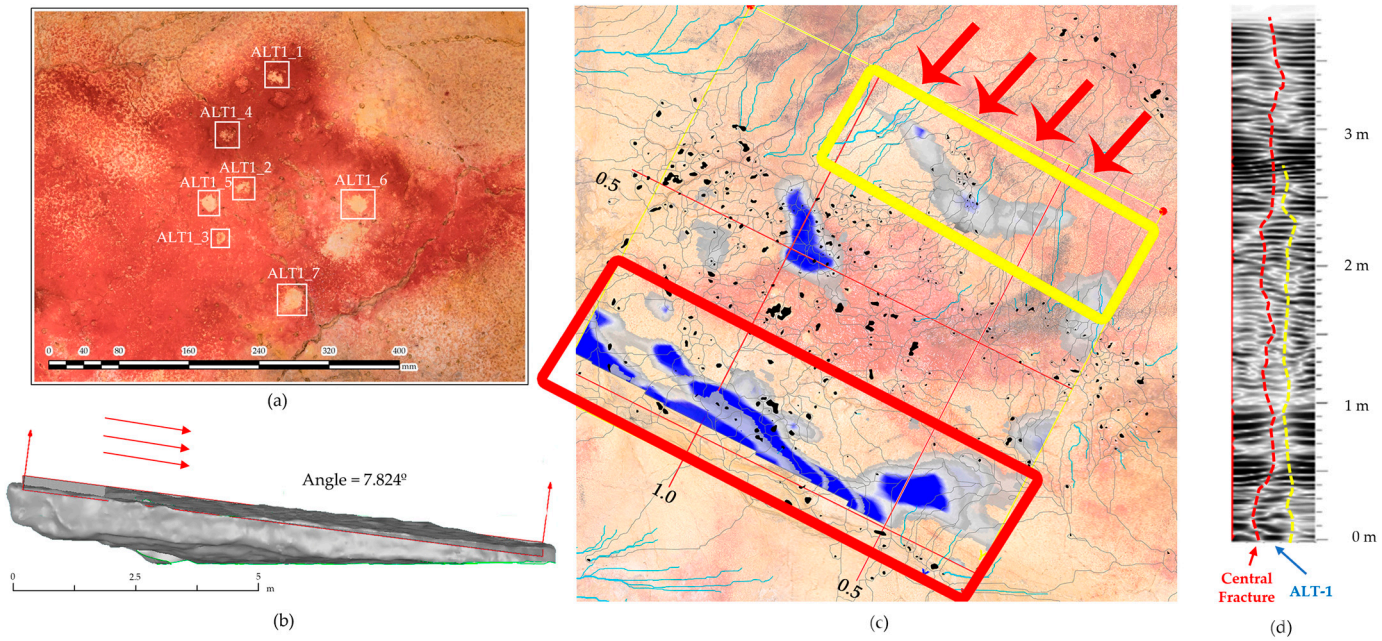

Figure 16. (**a**) Location of the drip points within the control area ALT1. (**b**) Mean dip of the Polychrome Hall calculated from the 3D model (**c**) Moistures associated with two large vertically developing fractures in the Polychrome ceiling. The red box shows the moistures associated with the large central fracture, the yellow box shows the moisture zones coming from the fracture located in the polychrome bison. The red arrows as well as the degree of dip of the ceiling show the relationship of this with the moistures associated with the dripping points with migration and loss of pigment from ALT1. (**d**) Reflection profile P8 obtained with the 300 MHz antenna. The dashed red line indicates the fracture (central fracture) associated with the moisture shown in red, and the dashed yellow line corresponds to the fracture associated with the moisture marked in yellow in (**c**).

The greatest percolation of water is towards the north side of the large central rift, in a west-to-east direction. This direction of moisture flow is explained by the dip of the strata. The moisture that percolates through the central fracture flows toward the fracture from

the beginning (west) to the bottom of the Polychrome Hall (east). Additionally, the greater percolation of moisture in the western area of the quadrant studied (Figure 7), on both sides of the central crack, compared to the east, is because the cement mortar that seals the large central crack is in a worse state of conservation in this area.

First, the detection of subsurface features, including fractures, fissures and moisture accumulations, offers important clues regarding the geological and hydrological dynamics within the cave system. Fractures and fissures may show structural weaknesses in the limestone bedrock, which could influence the infiltration and circulation of groundwater. The observed moisture accumulations are probably associated with localized percolation of water through fractures and with hydrological interactions between overlying rock layers. These findings support previous studies highlighting the significance of geological discontinuities and hydrological pathways in controlling the distribution of moisture within karstic systems [78,79].

Second, the characterization of moisture dynamics provides valuable information on the spatial distribution and temporal variability of moisture content within the Polychrome Hall. The identification of distinct moisture zones and their association with geological features, such as fractures and microchannels, suggests complex moisture transport processes influenced by both structural controls and external hydrological inputs. These findings contribute to our understanding of ceiling hydrology and underscore the importance of considering both intrinsic and extrinsic factors in modeling moisture dynamics within karst landscapes [80,81].

Third, the mapping of geological interfaces, including the contact between the Polychrome Layer and underlying dolomitic formations, provides valuable insights into the stratigraphic architecture and depositional history of the cave deposits. The observed irregularities and discontinuities in the Dolomitic Layer suggest complex geological histories characterized by tectonic activity, sedimentary deposition, and diagenetic processes as other complementary studies such as Scanning Electron Microscopy analysis (SEM) shows. These findings align with earlier studies on ceiling stratigraphy, highlighting the utility of GPR as a non-invasive tool for subsurface imaging and geological mapping in karst environments [82,83].

The detection of subsurface features using GPR represents a significant advancement in understanding the geological and hydrological dynamics of the Cave of Altamira Polychrome Hall ceiling. The identification of fractures and fissures not only provides insights into the structural integrity of the cave but also offers clues about the pathways through which water may infiltrate and circulate within the subsurface environment. These findings follow existing research on karst hydrogeology, which emphasizes the role of geological discontinuities in controlling groundwater flow and cave formation [84]. Further investigations into the spatial distribution and temporal evolution of subsurface features using advanced geophysical techniques could yield valuable insights into the dynamic nature of karst landscapes and their response to environmental change.

The variations seen in moisture moisture zones between different depths and locations underscore the heterogeneous nature of moisture distribution within the cave environment, highlighting the need for comprehensive hydrological modeling approaches that account for both intrinsic and extrinsic factors [85,86]. Future research efforts could focus on integrating GPR data with hydrological models to improve predictions of cave moisture dynamics under different climatic scenarios and land use conditions.

The mapping of geological interfaces, particularly the contact between the Polychrome Layer and underlying dolomitic formations, offers valuable insights into the cave's stratigraphic architecture and paleoenvironmental history. The identification of irregularities and discontinuities in the Dolomitic Layer suggests complex geological processes that have shaped the cave over geological timescales. These findings contribute to our understanding of cave formation mechanisms and provide a basis for reconstructing past environmental conditions [48,87]. The mechanisms of geological formation of the cave and the stratigraphic relationship with the Dolomitic Layer are significant areas of ongoing discussion.

The influence of this Dolomitic Layer on the conservation of the art on the ceiling is still to be fully explored, as it exerts a protective effect due to its lower permeability regarding the water located at higher depths. The aforementioned erosive processes cause its partial disintegration, increasing water access to the surface of the ceiling and escalating the risks of migration, disintegration and occasional washing away of the paintings. Future studies could use interdisciplinary approaches, combining GPR with sedimentological, geochemical and chronological analyses to unravel the intricate geological histories preserved within cave deposits.

5. Conclusions

This comprehensive study conducted in the Polychrome Hall of the Altamira Cave system has not only shed light on the complex subsurface features but has also highlighted the significance of employing advanced GPR techniques in cave research. By digging into the intricate geological and hydrological dynamics, this study has provided invaluable insights into the intricate karst landscape and cave ecosystem.

The detection and characterization of subsurface features such as fractures and geological interfaces offer a deeper understanding of the ceiling structural complexity and hydrological connectivity. These findings not only contribute to the scientific understanding of karst landscapes but also hold practical implications for cave management and conservation efforts.

The mapping of moisture dynamics within the cave system is noteworthy, as it provides essential information for managing cave microclimates, understanding speleothem formation processes and preserving cave ecosystems.

The interdisciplinary nature of this study underscores the importance of collaboration between managers of the cave addressing the challenges faced by karst landscapes. By integrating scientific research with conservation efforts and policymaking, we can work towards sustainable cave management practices that ensure the long-term preservation of these unique ecosystems.

This being a first approximation and considering the need to obtain new data for different periods, it can be affirmed, based on the studies conducted, that there is a dynamic of water infiltration which, through fractures, fissures and internal stratification planes, percolates down to the surface of the ceiling. The internal moisture zones mapped in our control area ALT1 on 17 February 2022 affected the washing of pigment from some drip points in this zone by April of the same year, as well as provoking the migration of paint in other associated drip points. The moisture recorded in April 2023 at a depth of 9 cm and above is expected to directly contribute to paint wash-off at the same drip points, and possibly others, by April 2024.

This leads us to a clear reflection: within barely nine months, the moisture level involved in pigment carry-over at our ALT1 drip points will be located a few centimeters from the ceiling surface, initiating new processes of paint carry-over and destruction a month and a half later. This specific pattern highlights a seasonal dynamic in the processes of water infiltration percolation, which directly affects the conservation of the paint. If this pattern is confirmed, it would open the door to determining or suggesting conservation actions at certain critical times of the year. These actions could address the access of water that generates the washing and migration of pigment, potentially reversing the ongoing deterioration.

While this study has provided valuable insights into the subsurface characteristics and moisture dynamics of the Polychrome Hall in Altamira Cave, future research is essential to improve conservation efforts. Long-term monitoring of moisture infiltration and moisture zones using advanced GPR techniques alongside non-invasive methods such as high-resolution photogrammetry will help to track seasonal variations that affect pigment preservation. Extending the study beyond the ALT1 control area will provide a broader understanding of hydrological dynamics and identify additional areas at risk. The development of predictive models based on observed water infiltration patterns can guide

timely conservation measures. In addition, collaboration with conservation experts will be essential to translate research findings into actionable strategies. Finally, investigating the potential impacts of climate change on cave ecosystems will be important to anticipate shifts in water infiltration that may exacerbate paint deterioration, to refine our understanding and improve conservation strategies for Cave of Altamira.

Author Contributions: Conceptualization, V.B., F.G. and A.P.; methodology, V.B., F.G. and A.P.; software, V.B. and F.G.; validation, C.D.L.H., F.G. and A.P.; formal analysis, V.B., F.G. and A.P.; investigation, V.B., F.G. and A.P.; resources, V.B. and P.F.; data curation, V.B. and F.G.; writing—original draft preparation, V.B., F.G. and A.P.; writing—review and editing, V.B., F.G. and A.P.; visualization, V.B. and F.G.; supervision, V.B., A.P. and C.D.L.H.; project administration, V.B., C.D.L.H. and P.F.; funding acquisition, V.B., C.D.L.H. and P.F. All authors have read and agreed to the published version of the manuscript.

Funding: This research was funded by the Department of Innovation, Industry, Tourism, and Trade of the Regional Government of Cantabria in the context of aid to encourage industrial research and innovation in companies, project "SImulador Climático del Karst de cuevas de especial valor. (SICLIKA)", grant number 2016/INN/25.

Data Availability Statement: The research data supporting this publication are not publicly available. The data were collected by GIM Geomatics as part of research and conservation studies of the Cave. These data are kept in the Museo Nacional y Centro de Investigación de Altamira. A video showing the results of this study is available in: https://youtu.be/dv82eE-r-iA, accessed on 18 October 2024.

Acknowledgments: The authors of this work would like to thank the GIM Geomatics company for its support of the project and, especially, J. Herrera.

Conflicts of Interest: The authors declare no conflicts of interest.

References

1. Hoyos, M.; Soler, V.; Cañaveras, J.C.; Sánchez-Moral, S.; Sanz-Rubio, E. Microclimatic characterization of a karstic cave: Human impact on microenvironmental parameters of a prehistoric rock art cave (Candamo Cave, northern Spain). *Environ. Geol.* **1998**, *33*, 231–242. [CrossRef]
2. Hoyos, M.; Bustillo, A.; García, A.; Martin, C.; Ortiz, R.; Suazo, C. *Características Geológico-Kársticas de la Cueva de Altamira (Santillana del Mar, Santander)*; Informe Ministerio de Cultura: Madrid, Spain, 1981; 81p.
3. Sánchez-Moral, S.; Cuezva, S.; Fernández Cortés, Á.; Janices, I.; Benavente, D.; Cañaveras, J.C.; González Grau, J.M.; Jurado, V.; Laiz Trobajo, L.; de Portillo Guisado, M.; et al. *Estudio Integral del Estado de Conservación de la Cueva de Altamira y su Arte Paleolítico (2007–2009). Perspectivas Futuras de Conservación*; Monografías del Museo Nacional y Centro de Investigación de Altamira, No. 24; Ministerio de Educación, Cultura y Deporte: Madrid, Spain, 2014.
4. Ministerio de Cultura y Deporte; Universidad de Cantabria; CSIC, Universidad del País Vasco; de Guichen, G. *Programa de Investigación Para la Conservación Preventiva y Régimen de Acceso de la Cueva de Altamira (2012–2014)*; Ministerio de Cultura y Deporte: Madrid, Spain, 2014; Volume II.
5. Ontañon, R.; Bayarri, V.; Herrera, J.; Gutierrez, R. The conservation of prehistoric caves in Cantabria, Spain. In *The Conservation of Subterranean Cultural Heritage*; CRC Press/Balkema: Boca Raton, FL, USA; Taylor & Francis Group: London, UK, 2014; ISBN 978-1-315-73997-7.
6. Bayarri, V.; Sebastián, M.A.; Ripoll, S. Hyperspectral Imaging Techniques for the Study, Conservation and Management of Rock Art. *Appl. Sci.* **2019**, *9*, 5011. [CrossRef]
7. Bayarri, V.; Castillo, E.; Ripoll, S.; Sebastián, M.A. Improved Application of Hyperspectral Analysis to Rock Art Panels from El Castillo Cave (Spain). *Appl. Sci.* **2021**, *11*, 1292. [CrossRef]
8. Teira, L.; Bayarri, V.; Ontañón, R.; Castillo, E.; Arias, P. Geometric and radiometric recording of prehistoric graphic expression: The case of Peña Tu (Asturias, Spain). *Archaeol. Anthr. Sci.* **2024**, *16*, 32. [CrossRef]
9. Bayarri, V.; Latova, J.; Castillo, E.; Lasheras, J.A.; De Las Heras, C.; Prada, A. Nueva documentación y estudio del arte empleando técnicas hiperespectrales en la Cueva de Altamira. In *ARKEOS | Perspectivas em Diálogo, Nº 37, Proceedings of XIX International Rock Art Conference IFRAO 2015: Symbols in the Landscape: Rock Art and its Context, Cáceres, Spain, 31 August–4 September 2015*; Conference Proceedings; Instituto Terra e Memória: Tomar, Portugal, 2015; ISBN 978-84-9852-463-5.
10. Ferrero, A.; Godio, A.; Sambuelli, L. Geophysical and Geomechanical Investigations Applied to the Rock Mass Characterisation for Distinct Element Modelling. *Rock Mech. Rock Eng.* **2007**, *40*, 603–622. [CrossRef]
11. Walton, G.; Lato, M.; Anschütz, A.; Perras, M.A.; Diederichs, M.S. Non-invasive detection of fractures, fracture zones, and rock damage in a hard rock excavation—Experience from the Äspö Hard Rock Laboratory in Sweden. *Eng. Geol.* **2015**, *196*, 210–221. [CrossRef]

12. Longoni, L.; Arosio, D.; Scaioni, M.; Papini, M.; Zanzi, L.; Roncella, R.; Brambilla, D. Surface and subsurface non-invasive investigations to improve the characterization of a fractured rock mass. *J. Geophys. Eng.* **2012**, *9*, 461–472. [CrossRef]
13. Arjwech, R.; Everett, M.; Chaisuriya, S.; Youngme, W.; Rattanawannee, J.; Saengchomphu, S.; Thitimakorn, T.; Somchat, K. Electrical resistivity tomographic detection of the hidden Thakek fault, Northeast Thailand. *Near Surf. Geophys.* **2021**, *19*, 489–501. [CrossRef]
14. Muhammad, H.; Yanjun, S. Hard-rock investigation using a non-invasive geophysical approach. *J. Appl. Geophys.* **2022**, *206*, 104808. [CrossRef]
15. Chalikakis, K.; Plagnes, V.; Guerin, R.; Valois, R.; Bosch, F.P. Contribution of geophysical methods to karst-system exploration: An overview. *Hydrogeol. J.* **2011**, *19*, 1169–1180. [CrossRef]
16. Pueyo-Anchuela, O.; Casas-Sainz, A.M.; Soriano, M.A.; Pocoví-Juan, A. A geophysical survey routine for the detection of doline areas in the surroundings of Zaragoza (NE Spain). *Eng. Geol.* **2010**, *114*, 382–396. [CrossRef]
17. Ezersky, M.; Bruner, I.; Keydar, S.; Trachtman, P.; Rybakov, M. Integrated study of the sinkhole development site on the western shores of the Dead Sea using geophysical methods. *Near Surf. Geophys.* **2006**, *4*, 335–343. [CrossRef]
18. Martínez-Moreno, F.J.; Galindo-Zaldívar, J.; Pedrera, A.; Teixido, T.; Ruano, P.; Peña, J.A.; Martín-Rosales, W. Integrated geophysical methods for studying the karst system of Gruta de las Maravillas (Aracena, Southwest Spain). *J. Appl. Geophys.* **2014**, *107*, 149–162. [CrossRef]
19. Kruse, S.E.; Grasmueck, M.; Weiss, M.; Viggiano, D. Sinkhole Structure Imaging in Covered Karst Terrain. *Geophys. Res. Lett.* **2006**, *33*, L16405. [CrossRef]
20. Samyn, K.; Mathieu, F.; Bitri, A.; Nachbaur, A.; Closset, L. Integrated geophysical approach in assessing karst presence and sinkhole susceptibility along flood-protection dykes of the Loire River, Orléans, France. *Eng. Geol.* **2014**, *183*, 170–184. [CrossRef]
21. Grasmueck, M.; Quintà, M.C.; Pomar, K.; Eberli, G.P. Diffraction imaging of subvertical fractures and karst with full-resolution 3D Ground-Penetrating Radar. *Geophys. Prospect.* **2013**, *61*, 907–918. [CrossRef]
22. Medeiros, W.E.; Oliveira, J.G.; de Santana, F.; Bezerra, F.; Cazarin, C. Enhancing Stratigraphic and Structural Features in GPR Images of Limestone Karst through Adequate Data Processing. In Proceedings of the 24th European Meeting of Environmental and Engineering Geophysic, Porto, Portugal, 9–12 September 2018. [CrossRef]
23. Bermejo, L.; Ortega, A.I.; Parés, J.M.; Campaña, I.; Bermúdez de Castro, J.M.; Carbonell, E.; Conyers, L.B. Karst features interpretation using ground-penetrating radar: A case study from the Sierra de Atapuerca, Spain. *Geomorphology* **2020**, *367*, 107311. [CrossRef]
24. Pipan, M.; Baradello, L.; Forte, E.; Prizzon, A. GPR study of bedding planes, fractures and cavities in limestone. In Proceedings of the 8th International Conference on Ground Penetrating Radar, Gold Coast, Australia, 23–26 May 2000. [CrossRef]
25. Neal, A.; Grasmueck, M.; McNeill, D.F.; Viggiano, D.A.; Eberli, G.P. Full-Resolution 3D Radar Stratigraphy of Complex Oolitic Sedimentary Architecture: Miami Limestone, Florida, U.S.A. *J. Sediment. Res.* **2008**, *78*, 638–653. [CrossRef]
26. Jeannin, M.; Garambois, S.; Grégoire, C.; Jongmans, D. Multiconfiguration GPR measurements for geometric fracture characterization in limestone cliffs (Alps). *Geophysics* **2006**, *71*, B85–B92. [CrossRef]
27. Batayneh, A.; Abueladas, A.; Moumani, K. Use of Ground-Penetrating Radar for Assessment of Potential Sinkhole Conditions: An Example from Ghor al Haditha Area, Jordan. *Environ. Geol.* **2002**, *41*, 977–983. [CrossRef]
28. García-García, F.; Valls-Ayuso, A.; Benlloch-Marco, J.; Valcuende-Payá, M. An optimization of the work disruption by 3D cavity mapping using GPR: A new sewerage project in Torrente (Valencia, Spain). *Constr. Build. Mater.* **2017**, *154*, 1226–1233. [CrossRef]
29. Reis, J.A.; Castro, D.L.; Jesus, T.E.; Filho, F.P. Characterization of collapsed paleocave systems using GPR attributes. *J. Appl. Geophys.* **2014**, *103*, 43–56. [CrossRef]
30. Gao, Q.; Wang, S.; Peng, T.; Peng, H.; Oliver, D.M. Evaluating the structure characteristics of epikarst at a typical peak cluster depression in Guizhou plateau area using ground penetrating radar attributes. *Geomorphology* **2020**, *364*, 107015. [CrossRef]
31. Allroggen, N.; Heincke, B.; Koyan, P.; Wheeler, W.; Rønning, J. 3D GPR attribute classification: A case study from a paleokarst breccia pipe in the Billefjorden area on Spitsbergen, Svalbard. *Geophysics* **2022**, *87*, WB19–WB30. [CrossRef]
32. Xu, S.; Sirieix, C.; Ferrier, C.; Lacanette-Puyo, D.; Riss, J.; Malaurent, P. A Geophysical Tool for the Conservation of a Decorated Cave—A Case Study for the Lascaux Cave. *Archaeol. Prospect.* **2015**, *22*, 283–292. [CrossRef]
33. Hœrlé, S.; Huneau, F.; Salomon, A.; Denis, A. Using the ground-penetrating radar to assess the conservation condition of rock-art sites. *Comptes Rendus. Geosci.* **2007**, *339*, 536–544. [CrossRef]
34. Denis, A.; Huneau, F.; Hœrlé, S.; Salomon, A. GPR data processing for fractures and flakes detection in sandstone. *J. Appl. Geophys.* **2009**, *68*, 282–288. [CrossRef]
35. Huneau, F.; Hoerlé, S.; Denis, A.; Salomon, A. First use of geological radar to assess the conservation condition of a South African rock art site: Game Pass Shelter (KwaZulu-Natal). *S. Afr. J. Sci.* **2008**, *104*, 251–254.
36. Bayarri, V.; Prada, A.; García, F.; Díaz-González, L.M.; De Las Heras, C.; Castillo, E.; Fatás, P. Integration of Remote-Sensing Techniques for the Preventive Conservation of Paleolithic Cave Art in the Karst of the Cave of Altamira. *Remote Sens.* **2023**, *15*, 1087. [CrossRef]
37. Bayarri, V.; Prada, A.; García, F. A Multimodal Research Approach to Assessing the Karst Structural Conditions of the Ceiling of a Cave with Palaeolithic Cave Art Paintings: Polychrome Hall at Cave of Altamira (Spain). *Sensors* **2023**, *23*, 9153. [CrossRef]
38. Bayarri, V.; Prada, A.; García, F.; De Las Heras, C.; Fatás, P. A Multisensory Analysis of the Moisture Course of the Cave of Altamira (Spain): Implications for Its Conservation. *Remote Sens.* **2024**, *16*, 197. [CrossRef]

39. Bayarri, V.; Prada, A.; García, F.; De Las Heras, C.; Fatás, P. Remote Sensing and Environmental Monitoring Analysis of Pigment Migrations in Cave of Altamira's Prehistoric Paintings. *Remote Sens.* **2024**, *16*, 2099. [CrossRef]
40. Pérez Gracia, V.; Di Capua, D.; González-Drigo, R.; Pujades, L. Laboratory characterization of a GPR antenna for high-resolution testing: Radiation pattern and vertical resolution. *NDT E Int.* **2009**, *42*, 336–344. [CrossRef]
41. Apel, D.B.; Dezelic, V. Evaluation of high frequency ground penetrating radar (GPR) in mapping strata of dolomite and limestone rocks for ripping technique. *Int. J. Surf. Min. Reclam. Environ.* **2005**, *19*, 260–275. [CrossRef]
42. Tosti, F.; Bianchini, L.C.; Calvi, A.; Alani, A.M.; Benedetto, A. An investigation into the railway ballast dielectric properties using different GPR antennas and frequency systems. *NDT E Int.* **2018**, *93*, 131–140. [CrossRef]
43. Rial, F.; Pereira, M.; Lorenzo, H.; Arias, P.; Novo, A. Resolution of GPR bowtie antennas: An experimental approach. *J. Appl. Geophys.* **2009**, *67*, 367–373. [CrossRef]
44. Bi, V.; Zhao, Y.; Shen, R.; Li, B.; Hu, S.; Ge, S. Multi-frequency GPR data fusion and its application in NDT. *NDT E Int.* **2020**, *115*, 102289. [CrossRef]
45. Fang, L.; Yang, F.; Xu, M.; Liu, F. Research on Development 3D Ground Penetrating Radar Acquisition and Control Technology for Road Underground Diseases with Dual-Band Antenna Arrays. *Sensors* **2023**, *23*, 8301. [CrossRef]
46. Conyers, L.B. *Interpreting Ground-Penetrating Radar for Archaeology*, 1st ed.; Left Coast Press Inc.: Walnut Creek, CA, USA, 2012; p. 220.
47. Pérez-Gracia, V.; García García, F.; Rodriguez Abad, I. GPR evaluation of the damage found in the reinforced concrete base of a block of flats: A case study. *NDT E Int.* **2008**, *41*, 341–353. [CrossRef]
48. Hoyos, M. Procesos de alteración de soporte y pintura en diferentes cuevas con arte rupestre del norte de España: Santimamiñe, Arenaza, Altamira y Llonín. In *La Protección y Conservación del Arte Rupestre Paleolítico*; Principado de Asturias: Oviedo, Spain, 1993; pp. 51–74.
49. TOPCON. Topcon Hyper II GNSS Receiver Specifications. Available online: https://pdf.directindustry.com/pdf/topcon/hiperii/22494-445419.html (accessed on 16 October 2024).
50. Leick, A.; Rapoport, L.; Tatarnikov, D. *GPS Satellite Surveying*, 4th ed.; John Wiley & Sons: New York, NY, USA, 2015.
51. Teunissen, P.; Khodabandeh, A. Review and principles of PPP-RTK methods. *J. Geod.* **2015**, *89*, 217–240. [CrossRef]
52. TOPCON. Topcon GPT. Available online: https://geodesical.com/es/pdfs/manuales/topcon-manual-estacion-total-serie-gpt-750-y-7500.pdf (accessed on 16 October 2024).
53. FARO. FARO Laser Scanner Focus 3D X 130 Technical Datasheet. Available online: https://downloads.faro.com/index.php/s/XYSMR89BwyD5fqg?dir=undefined&openfile=41913 (accessed on 8 February 2023).
54. Bayarri, V.; Castillo, E.; Ripoll, S.; Sebastián, M.A. Control of Laser Scanner Trilateration Networks for Accurate Georeferencing of Caves: Application to El Castillo Cave (Spain). *Sustainability* **2021**, *13*, 13526. [CrossRef]
55. Bayarri-Cayón, V.; Castillo, E. Caracterización geométrica de elementos complejos mediante la integración de diferentes técnicas geomáticas. Resultados obtenidos en diferentes cuevas de la Cornisa Cantábrica. In Proceedings of the VIII Semana Geomática Internacional, Barcelona, Spain, 3–5 March 2009.
56. Bayarri-Cayón, V.; Latova, J.; Castillo, E.; Lasheras, J.A.; De Las Heras, C.; Prada, A. Nueva ortoimagen verdadera del Techo de Polícromos de la Cueva de Altamira. In *ARKEOS | Perspectivas em Diálogo, Nº 37, Proceedings of the XIX International Rock Art Conference IFRAO 2015: Symbols in the Landscape: Rock Art and its Context, Cáceres, Spain, 31 August–4 September 2015*; Conference Proceedings; Instituto Terra e Memória: Tomar, Portugal, 2015; pp. 2308–2320.
57. Shweta, T.; Lakshi, R. Impact of GPR antenna height in estimating coal layer thickness using spatial smoothing techniques. *IET Sci. Meas. Technol.* **2020**, *14*, 906–912. [CrossRef]
58. Lei, Y.; Jiang, B.; Su, G.; Zou, Y.; Qi, F.; Li, B.; Jia, F.; Tian, T.; Qu, Q. Application of Air-Coupled Ground Penetrating Radar Based on F-K Filtering and BP Migration in High-Speed Railway Tunnel Detection. *Sensors* **2023**, *23*, 4343. [CrossRef] [PubMed]
59. Oikonomopoulou, E.C.; Palieraki, V.A.; Sfikas, I.P.; Trezos, C.G. Reliability and limitations of GPR for identifying objects embedded in concrete–Experience from the lab. *Case Stud. Constr. Mater.* **2022**, *16*, e00898. [CrossRef]
60. Jol, H.M. *Ground Penetrating Radar Theory and Applications*, 1st ed.; Elsevier Science: Amsterdam, The Nethrlands, 2009; p. 544.
61. Schmalholz, J.; Stoffregen, H.; Kemna, A.; Yaramanci, U. Imaging of water content distributions inside a lysimeter using GPR tomography. *Vadose Zone J.* **2004**, *3*, 1106–1115. [CrossRef]
62. Conyers, L.B. *Ground-Penetrating Radar for Archaeology*, 4th ed.; Rowman and Littlefield Publishers, Alta Mira Press: Lanham, MD, USA, 2023; p. 264.
63. Reynolds, J.M. *An Introduction to Applied and Environmental Geophysics*, 2nd ed.; Wiley-Blackwell, John Wiley & Sons Ltd.: Oxford, UK, 2011; p. 710.
64. Neal, A. Ground-Penetrating Radar and Its Use in Sedimentology: Principles, Problems and Progress. *Earth-Sci. Rev.* **2004**, *66*, 261–330. [CrossRef]
65. Martínez-Garrido, M.I.; Fort, R.; Gómez-Heras, M.; Valles-Iriso, J.; Varas-Muriel, M.J. A comprehensive study for moisture control in cultural heritage using non-destructive techniques. *J. Appl. Geophys.* **2018**, *155*, 36–52. [CrossRef]
66. Theune, U.; Rokosh, D.; Sacchi, M.D.; Schmitt, D.R. Mapping fractures with GPR: A case study from Turtle Mountain. *Geophysics* **2006**, *71*, B139–B150. [CrossRef]
67. Pipan, M.; Forte, E.; Guangyou, F.; Finetti, I. High resolution GPR imaging and joint characterization in limestone. *Near Surf. Geophys.* **2003**, *1*, 39–55. [CrossRef]

68. Lunt, I.A.; Hubbard, S.S.; Rubin, Y. Soil moisture content estimation using ground-penetrating radar reflection data. *J. Hydrol.* **2005**, *307*, 254–269. [CrossRef]
69. Fechner, T.; Yaramanci, U. Influence of complex dielectric properties on the characteristics of radar reflections. *Eur. J. Environ. Eng. Geophys.* **1996**, *1*, 287–301.
70. Sénéchal, P.; Perroud, H.; Sénéchal, G. Interpretation of reflection attributes in a 3-D GPR survey at Vallée d'Ossau, western Pyrenees, France. *Geophysics* **2000**, *65*, 1435–1445. [CrossRef]
71. McClymont, A.F.; Green, A.G.; Streich, R.; Horstmeyer, H.; Tronicke, J.; Nobes, D.C.; Pettinga, J.R.; Campbell, J.K.; Lan-gridge, R.M. Visualization of active faults using geometric attributes of 3D GPR data: An example from the Alpine Fault Zone, New Zealand. *Geophysics* **2008**, *73*, 11–23. [CrossRef]
72. Daniels, D.J. *Ground Penetrating Radar*, 2nd ed.; IEE Radar, Sonar and Navigation Series 15 (Ed.); The Institution of Electrical Engineers: London, UK, 2004; p. 752. [CrossRef]
73. Geophysical Survey Systems, Inc. GSSI. RADAN 7.6 Software. Available online: https://www.geophysical.com/software/ (accessed on 12 July 2024).
74. Benedetto, A.; Tosti, F.; Bianchini Ciampoli, L.; D'Amico, F. An overview of ground-penetrating radar signal processing techniques for road inspections. *Signal Process.* **2017**, *132*, 201–209. [CrossRef]
75. Nardino, M.; Prada-Freixedo, A.; Famulari, D.; Brilli, L.; Cavaliere, A.; Carotenuto, F.; Chieco, C.; Gioli, B.; Giordano, T.; Martelli, F.; et al. Intensive campaign on continuous isotopic sampling for environmental criticality in the Stalactites cave of Altamira karst. In Proceedings of the Science and Art IX, Science and Technology Applied to Heritage Conservation, Madrid, Spain, 17–19 October 2022; La Ciencia y el Arte IX; Ciencias y Tecnologías Aplicadas a la Conservación del Patrimonio. Ministerio de Cultura y Deporte: Madrid, Spain, 2023; pp. 159–170.
76. Cendrero, A. *Influencia de la Composición de la Roca Soporte en el Deterioro de las Pinturas de Altamira. Vol. Conmemorativo Cent. Altamira*; Dirección General del Patrimonio: Madrid, Spain, 1981; pp. 579–580.
77. Valle, F.J.; Moya, J.S.; Cendrero, A. *Estudio de la roca Soporte de las Pinturas Rupestres de la Cueva de Altamira. Zephyrus. XXVIII–XXIX*; Ediciones Universidad de Salamanca: Salamanca, Spain, 1978; pp. 5–15.
78. White, W.B. *Geomorphology and Hydrology of Karst Terrains*; Oxford University Press: New York, NY, USA, 1988; 464p.
79. Ford, D.C.; Williams, P.W. *Karst Hydrogeology and Geomorphology*; John Wiley & Sons: Hoboken, NJ, USA, 2007; 561p.
80. Yuan, D. Environmental and engineering problems of karst geology in China. In *Karst Hydrogeology: Engineering and Environmental Applications*; Beck, B.F., Wilson, W.L., Eds.; Balkema: Rotterdam, The Netherlands, 1987; pp. 1–11.
81. Olarinoye, T.; Gleeson, T.; Marx, V.; Seeger, S.; Adinehvand, R.; Allocca, V.; Andreo, B.; Apaéstegui, J.; Apolit, C.; Arfib, B.; et al. Global karst springs hydrograph dataset for research and management of the world's fastes flowing groundwater. *Sci. Data* **2020**, *7*, 59. [CrossRef]
82. Honings, J.P.; Wicks, C.M.; Brantley, S.T. Ground-Penetrating Radar Detection of Hydrologic Connectivity in a Covered Karstic Setting. *Hydrology* **2022**, *9*, 168. [CrossRef]
83. Busetti, A.; Calligaris, C.; Forte, E.; Areggi, G.; Mocnik, A.; Zini, L. Non-Invasive Methodological Approach to Detect and Characterize High-Risk Sinkholes in Urban Cover Evaporite Karst: Integrated Reflection Seismics, PS-InSAR, Leveling, 3D-GPR and Ancillary Data. A NE Italian Case Study. *Remote Sens.* **2020**, *12*, 3814. [CrossRef]
84. Lucas, D.; Fankhauser, K.; Maurer, H.; McArdell, B.; Grob, R.; Herzog, R.; Bleiker, E.; Springman, S.M. Slope Stability of a Scree Slope Based on Integrated Characterisation and Monitoring. *Water* **2020**, *12*, 447. [CrossRef]
85. Papageorgiou, E.; Foumelis, M.; Mouratidis, A. Earth Observation Data Synergy for the Enhanced Monitoring of Ephemeral Water Bodies to Anticipate Karst-Related Flooding. *GeoHazards* **2023**, *4*, 197–216. [CrossRef]
86. Lu, Q.; Liu, K.; Zeng, Z.; Liu, S.; Li, R.; Xia, L.; Guo, S.; Li, Z. Estimation of the Soil Water Content Using the Early Time Signal of Ground-Penetrating Radar in Heterogeneous Soil. *Remote Sens.* **2023**, *15*, 3026. [CrossRef]
87. Foyo, A.; Tomillo, C.; Sánchez, M.A.; Suarez, J.L. *Esquema Geológico del Entorno de la Cueva de Altamira*; Las-Heras, J.A., Ed.; Redescubrir Altamira, Turner: Madrid, Spain, 2002; pp. 273–286.